

**CASCADE FAILURE ANALYSIS OF ELECTRICAL
TRANSMISSION LINES USING ADINA**

by

© Aravind Siddam

A Thesis submitted to the

School of Graduate Studies

in partial fulfillment of the requirements for the degree of

Master of Engineering

Faculty of Engineering and Applied Sciences

Memorial University of Newfoundland

May, 2014

St. John's

Newfoundland and Labrador

ABSTRACT

Cascade failure of electrical transmission lines can be caused by a number of reasons. Dynamic forces like equipment failure, conductors rupture in any span, heavy wind loads, snow accumulation on conductors and structural members or ice shedding are known to be the main reasons for such a collapse. The primary objective of this investigation was to study the dynamic behavior of supporting towers, collapse of supporting towers and longitudinal dynamic maximum forces that were induced on the adjacent supporting towers due to conductors rupture in any span.

The study was performed on transmission lines, whose supporting towers were modeled with (a) Linear elastic truss and beam elements, (b) Moment-Curvature beam elements, with elastic-plastic material properties, and (c) Towers with load limiting devices or tower load controllers (TLC).

The transmission lines modeled with linear elastic truss and beam elements were used to perform the free vibration analysis to calculate the damping properties of the towers and the transmission lines. Each of these models was used to conduct static and transient dynamic analyses due to broken conductors in the middle span. The transient dynamic analyses were carried out with bare conductor (no-ice-loads) loading and 25-mm (1-inch) radial ice loading conditions.

The linear material models do not predict the failure or cascading of the transmission line towers, however considering the elements as moment-curvature beam models with elasto-plastic materials showed that the towers adjacent to the span, where conductors are ruptured, experienced large impact forces causing the adjacent towers to collapse. And the use of TLCs was able to limit the length of this cascade failure.

KEY WORDS: Transmission line modeling, Cascade Failure of towers, Moment-Curvature Beam Element, Tower Load Controller, Transient Dynamic Analyses

ACKNOWLEDGEMENTS

I take this opportunity to thank the Faculty of Engineering and Applied Sciences and the School of Graduate Studies, Memorial University of Newfoundland, for providing me this opportunity and the funds required to pursue this research.

I owe my deepest gratitude to my supervisor, Dr. Katna Munaswamy, for his guidance, motivation, useful remarks, and patience throughout the learning process of my Master's degree. Without his insight and persistent help, this dissertation would not have been possible.

I thank my extended family and friends for their generosity, well wishes and constant encouragement. Special thanks to Mr. T. L. Narasimhulu, Late. Mr. K. P. Rao and Drs. Sreenivas Rao and Sarada Ravinuthala.

Last, but not the least, none of this would have been possible without the love and support of my family. I dedicate this dissertation to my parents, Srinivasa Rao and Sailaja Siddam, and sister, Neena Devi Siddam, who have been the source of strength and belief throughout my life.

TABLE OF CONTENTS

Page

ABSTRACT	II
ACKNOWLEDGEMENTS.....	III
LIST OF TABLES.....	VI
LIST OF ILLUSTRATIONS	VIII
LIST OF SYMBOLS AND ABBREVIATIONS.....	IX
1.0 INTRODUCTION.....	1
1.1 SCOPE AND OBJECTIVE OF THE THESIS	6
1.2 THESIS LAYOUT	8
2.0 LITERATURE REVIEW	10
2.1 NUMERICAL MODELING AND ANALYSIS	11
2.2 PHYSICAL MODEL AND EXPERIMENTATION	13
2.3 SIMULATION AND NUMERICAL ANALYSIS.....	15
2.4 SUMMARY OF PREVIOUS WORK	20
3.0 MODELING SUPPORTING TOWERS AND TRANSMISSION LINE.....	21
3.1 MODELING OF GUYED-V STEEL LATTICE TOWER.....	21
3.2 MODELING OF SUPPORTING TOWER MEMBERS	30
3.3 CONDUCTOR MODELING	32
4.0 FREE VIBRATION ANALYSIS AND DAMPING	36
4.1 FREE VIBRATION ANALYSIS OF TOWER.....	36
4.2 FREE VIBRATION ANALYSIS OF TRANSMISSION LINE.....	39
4.3 DAMPING	41
5.0 STATIC AND TRANSIENT DYNAMIC ANALYSIS OF TRANSMISSION LINE WITH BROKEN CONDUCTOR	44
5.1 INITIAL STATIC ANALYSIS.....	44
5.2 BROKEN CONDUCTOR TRANSIENT DYNAMIC ANALYSIS	45
5.3 TRANSIENT DYNAMIC ANALYSIS FOR ICE-LOADED CONDUCTOR WHEN CONDUCTORS ARE RUPTURED	52
5.3.1 Ice Simulation on the Conductors.....	52
5.4 CLOSURE	58

6.0 ANALYSIS OF MOMENT-CURVATURE BEAM MODEL	60
6.1 MOMENT-CURVATURE BEAM ELEMENT MODEL	61
6.2 DETERMINATION OF MOMENT-CURVATURE RELATION FOR BEAM SECTION.....	62
6.3 DETERMINATION OF TORQUE-TWIST RELATION FOR BEAM SECTION.....	66
6.4 STATIC AND TRANSIENT DYNAMIC ANALYSIS OF TRANSMISSION LINE WITH BROKEN CONDUCTOR FOR LINE MODEL WITH MOMENT-CURVATURE ELEMENT.....	70
6.4.1 Transient Dynamic Analysis for Bare Conductor when Conductors are Ruptured	70
6.4.2 Transient Dynamic Analysis of transmission line with 1-in radial ice load on conductors with simulated conductor rupture in one of the span.....	76
6.5 CLOSURE	80
7.0 USE OF LOAD LIMITING DEVICES	82
7.1 ANALYSES OF INTACT TOWERS	84
7.2 COLLAPSE ANALYSIS OF TRANSMISSION LINE MODEL WITH TLC	90
7.2.1 Dynamic Analysis of Transmission Line Model with Bare Conductors.....	90
7.2.2 Dynamic Analysis of Transmission Line Model with 25mm (1-inch) Radial Ice Load	91
7.3 CLOSURE	94
8.0 CONCLUSION	96
9.0 RECOMMENDATIONS FOR FUTURE WORK.....	98
REFERENCES.....	i

LIST OF TABLES

	<u>Page</u>
Table 3-1	Conductor Characteristics of the Transmission Line..... 33
Table 4-1	Frequencies of Significant Twisting and Bending Modes in the Towers..... 37
Table 4-2	Natural Frequencies of Transmission Line Systems..... 39
Table 5-1	Maximum Dynamic Tensions in Insulator Strings on Adjacent Towers..... 51
Table 5-2	Maximum Dynamic Tensions in Insulator Strings on Adjacent Towers..... 57
Table 6-1	Moment-Curvature data for Section L64x64x4.8 with an axial force of 50 kN 65
Table 6-2	Torsional Moment-Angle of Twist data for Section L64x64x4.8 with an axial force of 50kN 69
Table 6-3	Maximum Dynamic Tensions in Insulator Strings on Adjacent Towers..... 72
Table 6-4	Maximum Dynamic Tensions in Insulator Strings on Adjacent Towers..... 78
Table 6-5	Tower Failure Time for the Adjacent Towers after Conductor Rupture 79
Table 7-1	Comparison of the Tension in Insulator Strings of the Truss Model with Bare Conductor 85
Table 7-2	Comparison of the Tension in Insulator Strings of the Truss Model with 25 mm (i-in.) radial Ice Loaded Conductor 86
Table 7-3	Comparison of the Tension in Insulator Strings of the Linear Material Beam Model with Bare Conductors 87
Table 7-4	Comparison of the Tension in Insulator Strings of the Linear Material Beam Model with Ice Loaded Conductors..... 88
Table 7-5	Maximum Insulator Forces in Adjacent Towers in M-C Beam Model with ... Bare Conductors..... 91
Table 7-6	Maximum Insulator Forces in Adjacent Towers in M-C Beam Model with ... Ice Loaded Conductors 93

LIST OF ILLUSTRATIONS

	<u>Page</u>
Figure 1.1 Broken Conductors and Tower Failure due to the 1998 Storm in Montreal	3
Figure 1.2 A Collapsed Power Pylon due to 1998 Storm	4
Figure 1.3 V-Type Guyed Tower.....	6
Figure 3.1 Elevation view of Guyed-V Steel Lattice Tower	22
Figure 3.2 Bottom Mast Guyed-V Steel Lattice Tower.....	23
Figure 3.3 Top Mast of Guyed-V Steel Lattice Tower	24
Figure 3.4 Extension 26.09 m (20 ft.) of the Guyed-V Steel Lattice Tower	25
Figure 3.5 Extensions 15 feet of the Guyed-V Steel Lattice Tower	26
Figure 3.6 Half Cross-arm of the Guyed-V Steel Lattice Tower.....	27
Figure 3.7 Vertical Mast of the Guyed-V Steel Lattice Tower.....	28
Figure 3.8 Symmetric Half of the Guyed-V Steel lattice Tower	29
Figure 3.9 Geometrical Guyed-V Tower (Isometric View).....	30
Figure 3.10 Section of the Finite Element Model of the Transmission Line Model	35
Figure 4.1 Mode 1 of the Transmission Tower.....	37
Figure 4.2 Mode 2 of the Transmission Tower.....	38
Figure 4.3 Mode 3 of the Transmission Tower.....	38
Figure 4.4 Mode 1 of the Transmission Line.....	40
Figure 4.5 Mode 2 of the Transmission Line.....	40
Figure 4.6 Mode 3 of the Transmission Line.....	41
Figure 5.1 Transmission Line Section in Static Equilibrium.....	46
Figure 5.2 Transmission Line Section after Conductor Rupture in one of the Span	47
Figure 5.3 Force at Insulator after Broken Conductor (Peyrot, Kluge and Lee, 1980) ...	47
Figure 5.4 Time History of Insulator Tension for the Insulators of Adjacent Towers to Conductor Rupture in Truss Model	49
Figure 5.5 Time History of Insulator Tension for the Insulators of Adjacent Towers to Conductor Rupture in Beam Model.....	50
Figure 5.6 Schematic Cross-sectional View of a Loaded Conductor	53
Figure 5.7 Time History of Insulator Tension for the Insulators of Adjacent Towers to Conductor Rupture in Truss Model	55
Figure 5.8 Time History of Insulator Tension for the Insulators of Adjacent Towers to Conductor Rupture in Beam Model	56
Figure 5.9 Members Identified in the Cross-arm of the First Adjacent Tower	58
Figure 6.1 ADINA Input Curves for the Moment-Curvature Models	61
Figure 6.2 Finite Element Model of Cross-Section L64x64x4.8 using the Plate	63
Figure 6.3 Deformed Configuration of the Beam Section due to Moment about Y-axis with an Axial Load.....	64

Figure 6.4	Moment-Curvature Relationship (data from Table 6.1) for Section L64x64x4.8	66
Figure 6.5	Finite Element Model of Cross-Section L64x64x4.8 using the 3D-Solid Element	67
Figure 6.6	Deformed Configuration of the Beam Section due to Torque about X-axis with an Axial Load.....	68
Figure 6.7	Torsional Moment-Angle of Twist Relationship (data from Table 6.1) for Section L64x64x4.8	69
Figure 6.8	Time History of Insulator Tension for the Insulators of Adjacent Towers to Conductor Rupture.....	71
Figure 6.9	Transmission Line Cascade Failure in Two Towers Adjacent to the Span where Conductor Rupture Occurs.....	73
Figure 6.10	Start of failure of members in the first tower adjacent to the span where conductor breakage occurs	74
Figure 6.11	First Adjacent Tower Complete Failure	74
Figure 6.12	Start of failure of members in the second tower adjacent to the span where conductor breakage occurs	75
Figure 6.13	Second Adjacent Tower Complete Failure.....	75
Figure 6.14	Time History of Insulator Tension for the Insulators of Adjacent Towers to Conductor Rupture.....	77
Figure 6.15	Transmission Line Cascade Failure in Eight Towers Adjacent to the Span where Conductor Rupture Occurs	80
Figure 7.1	Load-Deformation Characteristic of TLC	84
Figure 7.2	Time History Response of the Insulator Strings in Truss Line Model with Radial Ice Load	89
Figure 7.3	Time History Response of the Insulator Strings in Beam Line Model with Radial Ice Load	89
Figure 7.4	Force History of the Insulator String in the First Tower, adjacent to the Conductor Failure Span, of the Moment-Curvature Beam Line with TLC and Bare Conductors.....	90
Figure 7.5	Transmission Line Section with Radial Ice Load.....	92
Figure 7.6	Comparative Force History of the Insulator String in the First Tower, adjacent to the Conductor Failure Span, of the Moment-Curvature Beam Line (with and without TLC) with Radial Ice Load	94

LIST OF SYMBOLS AND ABBREVIATIONS

ADINA	Automatic Dynamic Incremental Non-linear Analysis
FEA	Finite Element Analysis
ACSR	Aluminum Conductor Steel Reinforced
ASCE	American Society of Civil Engineers
kN	Kilo Newtons
Sec	Seconds
Rad	Radians
mm	Millimeters
m	Meters
in	Inches
ft	Feet
[C]	Damping Matrix
[M]	Mass Matrix
[K]	Stiffness Matrix
ζ	Critical Damping Ratio
ω	Natural Frequency of the system at i^{th} mode of vibration
α and β	Rayleigh Damping Coefficients
TLC	Tower Load Controller

1. Introduction

A world without electricity is simply unimaginable in this modern era. It has become a quintessential part of our existence. In a day-to-day life, electricity is utilized to run just about every electrical and electronic appliance or machine. The world, as of today, would come to a halt without electric power. Hence, power transmission systems play a pivotal role in transporting power over long distances from power generating stations, which are generally located far away from densely populated regions and close to the source of fuel or energy.

Typical overhead transmission power lines are laid out in long straight sections along the roadside supported by supporting structures, thus bringing down the cost of construction to connect system supply point and substations. However, such a layout is more prone to cascading failure. Cascading failure occurs when one supporting tower collapses, it increase the forces on the adjacent or subsequent towers, giving rise to multiple tower failures. (Whiteway, 2005)

An electrical transmission line comprises of conductors attached to a series of power transmission towers, which consists of three main components, namely-

- Support structures or towers
- Insulator strings
- Conductors

The conductors are attached to the insulator strings, which are connected to the cross arm of supporting towers. A long straight section of power lines is formed by a series of

towers, maintaining the continuity of power transmission through the conductors. Failure of even a single component in this system can disrupt the flow of electricity causing power outage to the consumers. (Tucker, 2007)

All transmission lines are designed to endure primary loads (like wind gusts, ice loads or a combination of both) and secondary loads (like failure of the component, ice shedding or galloping). Primary loads can be specified from historic data and other assumptions, but secondary loads are not easy to predict, as they are more dynamic in nature. When a transmission line experiences heavy loading (example, due to snow storm), there is a large amount of strain energy stored in the conductor lines. Under the influence of this loading, if the conductor (or any other component) fails or ruptures, the strain energy released will cause dynamic impact loads on the support structures (Peyrot, 1980). Also, as the support structures reach equilibrium, they will experience an unbalanced residual longitudinal load that gives rise to the redistribution of forces in the conductor-structure system. If the adjacent structures cannot withstand these new redistributed forces, it may lead to cascading failure of these structures. (Munaswamy and Dunford, 2013)

Historically, cascading failures have caused significant economic loss and in some cases, loss of lives too. An example of such an infamous cascade failure occurred in 1998 during the North American Ice Storm, which left four million people without power for about a week in Quebec, New Brunswick and Ontario. It was estimated that at least twenty-five people lost their lives due to hypothermia (Wikipedia, 2013). That same year, Newfoundland experienced some terrible power outage. More recently, in December 2007 and January 2013 Newfoundland has seen prolonged power disruptions in many

areas that caused major economic losses to the province and local businesses. Figure 1.1 and Figure 1.2 illustrate some examples of the damage caused by the ice storm on transmission lines and their support structures.

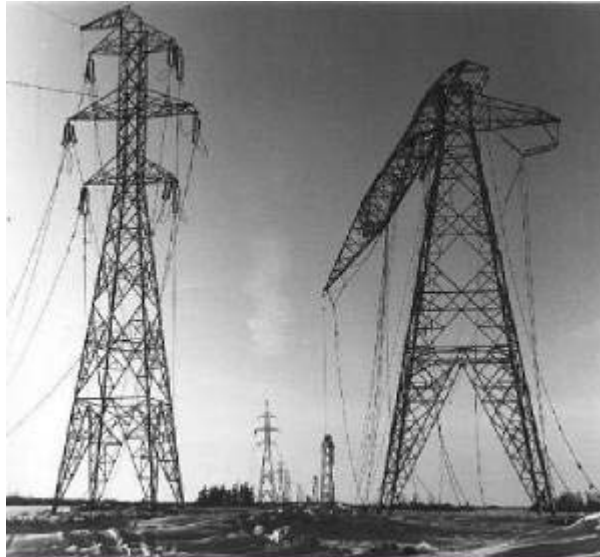


Figure 1.1 Broken Conductors and Tower Failure due to the 1998 Storm in Montreal

Source: <http://icestormof1998.tripod.com>



Figure 1.2 A Collapsed Power Pylon due to 1998 Storm

Source: <http://icestormof1998.tripod.com>

Similar cases of power outages were experienced in other countries as well. In October 2011, about two million people experienced blackout due to a severe snowstorm along the East Coast of the USA. Recently, in February 2013, more than 600,000 homes lost power due to the deadly blizzard (USA Today, 2013). In April 2008, the city of Szczecin, Poland experienced a total blackout. More than 400,000 residents were affected by this, as the city came to a standstill and the health care systems had to completely rely on generators (The Warsaw Voice, 2008).

All the above examples show a similar type of power line failure, caused by heavy ice/snow deposits and wind gusts. These are essentially primary loads, but have the tendency to become secondary loads by causing damage to a component or by ice shedding. In such cases, despite the primary loads being below the design value, the

secondary loads could cause substantial damage that may result in cascade failure. Therefore, in order to design better transmission power lines and to reduce the chances of a collapse, there is a need to understand the dynamic loads acting on the transmission system during cascading failure. This also helps in designing a better structure that takes premature failure of component into account. Furthermore, in many current design cases, the dynamic load effects are not considered directly, thus the post-failure force distribution remains unknown. Since the design process under secondary loads is very biased, it is important to understand the post-failure force distribution in a line to ensure proper strength coordination (Tucker and Haldar, 2007).

There have been many experiments and studies conducted to understand the dynamic behavior of transmission lines under longitudinal loading caused by ruptured/broken conductors. For this current investigation, a typical 230kV transmission line arrangement, made up of thirty guyed-V steel lattice towers, was used. A guyed tower is a tower that requires the use of guy wires to add stability to the tower structure. A typical guyed tower is shown in Figure 1.3. This type of tower can be divided into four parts, namely-

- Bottom mast
- Extension
- Top mast
- Cross-arm

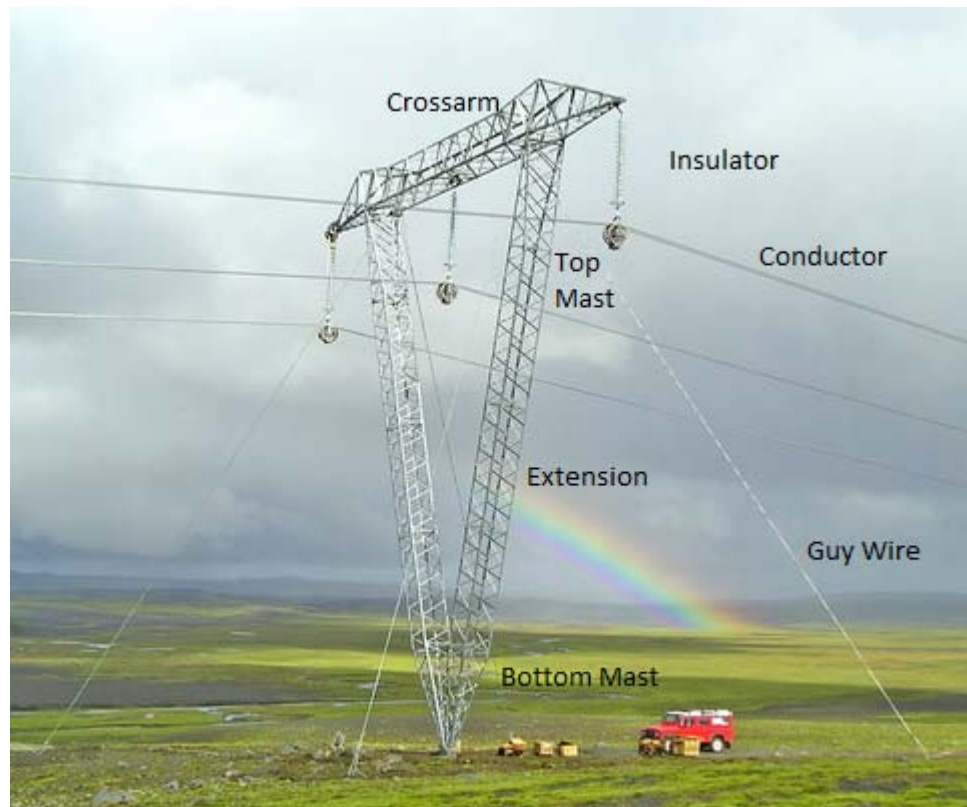


Figure 1.3 V-Type Guyed Tower
Source: www.mannvit.com

1.1 Scope and Objective of the Thesis

This present research was conducted to study the cascade failure of electrical transmission lines, subjected to longitudinal loads due to the conductors ruptured in one of the spans of a transmission line. The study was performed using ADINA (Automatic Dynamic Incremental Nonlinear Analysis) (ADINA, 2003). It is a commercial computer program that has been exclusively used in this study for finite element analysis of the transmission line system. “Although there are other commercial software available for the analysis of this type of problem, ADINA has been shown to be a valuable tool in

assessing the dynamic impact forces experienced by structures due to failed components.” (Tucker, 2007)

The main objectives of this study were:

- To study the dynamic behavior of supporting towers and dynamic forces that are acting on the adjacent supporting towers due to conductors ruptured in any span. These transmission line systems were studied under bare conductor (no-ice-load) and 25-mm (1-in) radial ice load conditions.
- To study the cascade failure of the towers due to broken conductors in one of the spans of the transmission line, under bare conductor and ice loading conditions. For this study, the members of the towers were modeled using Moment-Curvature beam model.
- To study the effect of load limiting devices in reducing the longitudinal loads on the towers and possible prevention of cascade failure.

For the current research, two modeling approaches have been used to model the tower of the transmission line.

- In the first approach, structural members of the tower were modeled using linear elastic bar element. In this model, all the components in the power line were considered to be truss elements; which included the conductors, insulators, guy wires and the members of the support structures.

- The second modeling approach utilized the beam element strategy, where all the members of the towers were modeled using beam elements, whereas the conductors, insulators and guy wires were taken as truss elements.

The dynamic behavior of transmission lines with both the modeling approaches were studied, by incorporating linear elastic and nonlinear elasto-plastic material properties for the transmission line towers.

1.2 Thesis Layout

Chapter 2 is the literature review section. There have been some very important investigations conducted in the past to understand the dynamic loading on transmission lines. This chapter is organized into three main sections; numerical modeling and analysis, physical modeling and experimentation, and simulation and numerical analysis. This chapter discusses significant studies conducted and documented since the 1960s, in brief.

Chapter 3 will specify the modeling process of transmission towers and the transmission line system. It details the steps involved in the development of the towers and line system. It also summarizes the two modeling approaches considered to conduct this research.

Chapter 4 details the free vibration analysis of towers and line systems. It also explains the Rayleigh damping criteria and shows how the damping coefficients have been calculated for the present investigation.

Chapter 5 presents the static and transient dynamic analyses of the intact structures. It presents the broken conductor transient dynamic analyses performed on the truss and beam transmission line models, with and without radial ice loading on the conductors. Additionally, the members in which the stresses exceed the yield strength will be identified in this chapter.

Chapter 6 will talk about the use of moment-curvature beam element in modeling the transmission line support structures. It details how the moment-curvature and torque-twisting relations were determined and how the modeling procedure was carried out to conduct this study. Furthermore, this chapter presents the cascade failure in the transmission line by performing a transient dynamic analysis, when the conductors (with and without the radial ice-load conditions) in one of the spans were made to fail.

Chapters 7 will discuss the use of load limiting devices and how the use of Tower Load Controller (TLC) can affect the cascade failure. All the transmission line models were redeveloped with the addition of TLCs and transient dynamic analyses were performed on each of these line models. The results obtained from these analyses were used to conduct a comparative study with respect to the previous models.

Chapter 8 summarizes the findings and concludes the thesis.

Chapter 9 will recommend the scope for future research in this field.

2. Literature Review

The history of transmission power lines dates back to the late 1800s. But, major studies to establish the safe design requirements for transmission towers started taking shape after World War II. Much of the research conducted until the late 1970s concentrated on proper modeling methodologies for transmission lines. Many mathematical and analytical models were presented until this period. But, there were very few full-scale field experiments due to the heavy costs involved. However, throughout the 1980s many people recognized the need for a better understanding of dynamic response of transmission lines. This gave rise to the formation of some very intricate modeling strategies and computer programs, which revolutionized and simplified the modeling process. As the computer programs evolved and became more complex, much of the research work started to focus on simulations and numerical modeling of transmission line systems, without actually having to conduct any full-scale field tests, thus saving a lot of costs incurred in conducting such tests. Lately, there are some very sophisticated commercial software applications available that could simulate the dynamic behavior and predict the responses of the transmission line systems very accurately that eased the procedure of designing more reliable power line systems.

Previously, transmission lines were made out of wood, but the design of transmission towers has evolved and today there are different kinds of metals and alloys used in the construction of transmission line systems that can handle up to 735kV of power. However, if there was one thing that has not changed since the early 20th century is the connection between the conductor and tower. Since these conductors are made up of

highly conducting metals and are protected by a thick insulator, they are very heavy and have large structural loads. (Tucker, 2007)

When these conductors break or rupture, large dynamic loads are generated. These loads could be transmitted from one tower to another, causing a chain event that could have disastrous effects on the line. Therefore, it is evident that dynamic loads pose a threat to the transmission system. A lot of research has been conducted in the past to make dependable transmission lines.

2.1 Numerical Modeling and Analysis

Lummis, J and Fiss, R (1969) presented a paper discussing the need to address the unbalanced longitudinal tensions in conductors. They suggested the use of tubular structures, rather than the conservative and rigid latticed-steel structures. Furthermore, they demonstrated mathematically the need for a more flexible structure, which can minimize loading imposed by the accidental failure of conductors. This shows that the support structures in a transmission tower will experience more stresses and are prone to complete failure when the structures are designed to show displacement in only one plane.

Lindsey, K. (1978) presented the first unified mathematical model to predict the longitudinal strength of a transmission line in 1978. The longitudinal loads considered included broken wires, unbalanced ice and extreme wind forces, which resulted in

structural deflection beyond the elastic limit. His model showed the use of elastic-plastic structure. The model was then compared to some experimental results and also, new results were demonstrated. This transmission system model was assumed to be a straight transmission line on a level terrain.

Roy *et al.* (1984) examined the secondary effects from the large displacements caused by flexible towers. They reviewed the secondary stresses in the rigid joints and member continuity. Also, they were able to test the reliability of tower strength predicted by the ASCE (American Society of Civil Engineers) design guidelines. They analyzed the structure using two iterative methods and by comparing them realized that it is not possible to treat a structure to single loading condition only, when the structure is assumed to be a planar joint, using the updated geometric method. However, using the initial stiffness method surpassed these limitations, with the implementation of an additional special technique. They then went on to study the effect of height of the towers on secondary stresses and found out that the stresses increase with height and flexibility.

Kahla (1993) described an equivalent beam-column based guyed mast. He presented equivalent properties for the triangular cross-section mast built-up patterns. His mathematical model was referred to as the approximate model. The guyed tower was modeled with three-dimensional beam elements. The tower was attached to cable elements and the connection between the tower and the cables was assumed rigid. He then mathematically performed a non-linear static analysis. Later, he compared the results obtained with an existing truss model. He was able to conclude that with the use of less nodes and elements, and careful designing of guyed towers as an equivalent beam-

column structure, the results obtained were in agreement with that of the truss element model.

2.2 Physical Model and Experimentation

Peyrot, Kluge and Lee (1980) conducted full-scale tests on a decommissioned electric transmission line to determine the maximum dynamic longitudinal forces, impact forces and residual forces on the towers adjacent to the span where the conductors were cut. They performed a series of tests, which included broken conductor tests and broken insulator tests. They even developed a new peak dynamic load prediction technique, which verified the full-scale tests. “The technique can also consider the effect of flexible structures to reduce the maximum loads.” (Peyrot, Kluge and Lee, 1980)

An outline of the design procedure for estimating the static and dynamic loads and the corresponding structural response due to rupture of wires was given by Mozer, Wood and Hribar (1981). In this paper, the results obtained from tests on a 345kV transmission line model were presented. It was noted that the measured structure impact factors for broken shield wire or dropped ice tests were less when compared to that of broken conductor tests. This emphasized the need to further relate the longitudinal loads determined in this test to the reliability of the transmission lines to withstand cascading failure.

Richardson (1987) conducted a model test to find a method to calculate flexibility of steel pole transmission lines. The results obtained by this small-scale test proved that structural

flexibility reduces dynamic and residual load on a transmission line system. For these tests, Richardson put together a 1:25 scale model of a transmission steel pole system with eleven spans. Then he applied various loading conditions, including a broken conductor, broken static wire, broken insulator, and ice unloading and galloping to study the longitudinal loadings on flexible transmission structures. He concluded that longitudinal loads were higher with long insulators and very high loads due to galloping on rigid structures. The results obtained in this experiment were useful to interpret the full-scale results.

Ostendorp (1998) identified the need and suggested a utilitarian method that can determine the magnitude of extreme event loads and assess the prospective cascading of a transmission line. For this study, he defined transmission line reliability levels using simplified risk assessment methods developed in Cascading Failure Risk Assessment (CASE) project. “The goal of the evaluation is to identify the first structure in the line that is capable of resisting all unbalanced longitudinal loads without failure.” (Ostendorp, 1998) Such a structure was defined as critical containment structure. He showed that empirically developed response coefficients were useful to define the dynamic characteristics of successive support structures.

Peabody and McClure (2002) discussed about the use of load limiters to reduce the dynamic forces on overhead line structures due to broken wires. They discussed the advantages and limitations of three types of load limiting devices namely- releasing and sliding clamps, insulator assembly releases and rotating and deformable cross-arms. They presented a brief summary on rotating and deformable cross-arms. Finally, they identified

and proposed the important characteristics that a load limiting device shall possess to find practical applicability.

2.3 Simulation and Numerical Analysis

Thomas and Peyrot (1982) proposed a numerical technique that produced broken conductor load histories for a conductor line. They used a typical time history, which showed variation of tension in a conductor of one span when ruptured, with respect to time. They utilized the test results from previous experiments to validate the results obtained analytically by a program, CABLE7. The paper outlined the algorithm of the program and also showed that the experimental data was very close to the analytical data calculated by the program. Additionally, the program output included summaries and plots of displacements and tensions for various line configurations.

Mathur et al. (1987) constructed several finite element models of a guyed transmission tower system, with two spans to present a free vibration analysis of the transmission line. The paper outlined the results of this analysis to give relative modal displacements for different components of the guyed tower. This numerical analysis consisted of a guyed Y-type tower made up of thirteen beam elements. The conductors and guy wires were taken as parabolic cable elements and the insulator was also modeled as a short beam element. Then the paper illustrated the mode shapes (both in-plane and out-plane) for the guyed towers and suggested that rather than attaching the conductors directly to the

tower, it was better to attach them to the insulators. This way the horizontal forces due to galloping could be significantly reduced.

McClure and Tinawi (1987) performed nonlinear dynamic analyses using ADINA with four existing small-scale model sections, subjected to conductor breakage. The basic model consisted of three towers and three conductors. They summarized the sources of nonlinearities under exceptional longitudinal loads. They evaluated the transient dynamic response due to conductor breakage. One of the models showed an identical behavior as the experimental model, but with some minor discrepancies identified by the authors, such as absence of damping for components and coarse meshing of poles. If these could be rectified, the authors believed that a real electric transmission line could be developed with this particular model as reference.

Gupta *et al.* (1994) simulated a real cascade failure of sixty-nine H-pole structures of a 345kV transmission line. The failure was caused due to an ice storm in Central Iowa in 1990. The paper documented the damage and performed a non-linear structural analysis using ETADS software. They modeled a finite element structure in the portion where they speculated the failure was initiated. About five structures were considered, with the main structure under consideration taking the center of the arrangement. This gave a better understanding of the behavior of the immediate structures too. After applying the dynamic loads, they were able to present sufficient data and enough reasons to provide valuable information for the designers to consider when designing transmission lines to withstand similar loads in future.

To understand the effect of transmission tower failure on the longitudinal loads acting on a simulated transmission line cascading condition, Kempner (1997) conducted several small scale model tests. He developed scaled models (1:23rd scale) to perform these tests. He studied effects of (a) Type of the tower, (b) Type of conductor, (c) Conductor initial tension, (d) Length of the insulator strings and (e) Span length, on cascading failure of the transmission lines, subjected to longitudinal loads.

Fekr and McClure (1998) simulated the dynamic effects of ice-shedding on overhead transmission lines with the help of a numerical model. The model was developed in ADINA, commercial non-linear FEA software. They considered about twenty-one different ice shedding load conditions in their study, with variable ice thickness, span length and insulator string length. They were able to determine the effects of these varying load conditions on the transmission line system. Even though the study neglected the wind effects and interaction between towers, it was useful in understanding the dynamic effects of ice-shedding on overhead transmission lines.

Madugula *et al.* (1998) presented a paper on the dynamic response of guyed masts. Guy masts are extensively used in telecommunications and they follow a similar behavior of transmission lines when subjected to longitudinal loads, especially ice loads. This was a very significant paper, as it discusses the use of truss-type of elements and beam-type of elements in designing guy masts. In this study, two models, of truss and beam respectively, were developed and their natural frequencies were determined. The results obtained were then compared to real guy masts of varying sizes to validate the effectiveness of various factors considered in this study. They utilized non-linear FEA

software ABAQUS to conduct the analysis. They found that the truss and beam element models were accurate, but the beam column element was proven to show appreciable savings in solution time.

McClure and Lapointe (2003) summarized a macroscopic modeling approach to transmission line dynamic analysis. They emphasized on studying the propagation of shock loads in a line section. They illustrated their macroscopic model with a case study of a double circuit 120kV line section. “The non-linear dynamic analyses performed utilize two and three-dimensional models of this line section.” (McClure and Lapointe, 2003). Also, their approach could be adapted to study ice-shedding effects from conductors or failure of line components. However, the major limitation of this model is that all the analyses were performed considering linear elastic materials, but in reality the transmission line members are non-linear in nature.

Majority of structural analysis done for telecommunication or transmission towers assume a simple truss behavior, which could compromise the assumed structural behavior. In 2005, da Silva *et al.* proposed an alternative structural analysis modeling strategy for the steel tower design. They used spatial truss finite elements, spatial beam finite elements and combined truss and beam three-dimensional finite elements. After developing the three models they performed static, dynamic and stability analysis on all the three model strategies and compared the results obtained to ascertain the advantages and limitations within each modeling approach. They found out that the maximum stress values differed by 30-47% from the usual truss modeling approach, but there was not much change with the lateral displacement values. In the free vibration analysis, they

found a 20% difference in the fundamental frequencies between the truss or beam model strategies and the combined approach. Finally, the paper concluded that a less conservative approach, the combined or mixed model strategy, can be used to design telecommunication or transmission towers. (da Silva *et al.*, 2005)

de Oliveira. M *et al.* (2007) performed the same analysis on guyed steel telecommunication towers for radio antennas. The analysis methodologies were the same as in da Silva et al, 2005, with the addition of non-linear analysis to the investigation. The numerical analysis was performed on ANSYS, commercial FEA software. They used three existing models of varying lengths and developed individual models for each model strategy approach. The results and conclusions obtained were similar, but they detected non-linearity under extreme load conditions.

Tucker (2007) studied the effect of insulator failure and conductor failure on cascading of a transmission line. A finite element model of the line was developed using three different element types to conduct this research. The insulator failure tests were carried out for varying ice loads with different insulator lengths and initial tensions. Conductor failure tests were performed to determine the peak dynamic forces acting on the surviving towers of the transmission line and comparing the results thus obtained to validate the data with experimental results.

Munaswamy and Dunford (2013) conducted a research to assess the peak dynamic and residual static loads on the supporting structure in a transmission line due to conductors rupture and to study the effects of flexibility of supporting structures in the transmission

line on maximum dynamic impact and residual conductor loads. They also performed a sensitivity analysis to study the effects of varying conductor tensions, ice loads, insulator string lengths and the type of terrain, on the peak dynamic and residual static loads.

2.4 Summary of Previous Work

Considerable amount of research effort has been directed to study the behavior of the towers under longitudinal loads for estimating the static and dynamic loads. There have been extensive studies, both analytical and experimental studies, to determine the maximum transient and residual longitudinal loads on towers due to broken conductor loads and component failure. But, these studies were focused to determine impact factors due to sudden rupture of conductors. It seems not much attention was given to cascade failure of transmission lines.

This present research was conducted to study the cascade failure of electrical transmission lines, subjected to longitudinal loads due to the conductors rupture in one of the spans of a transmission. The study is performed using ADINA (Automatic Dynamic Incremental Nonlinear Analysis) (ADINA, 2003). It is a commercial computer program that has been exclusively used in this study for finite element analysis of the transmission line system. “Although there are other commercial software available for the analysis of this type of problem, ADINA has been shown to be a valuable tool in assessing the dynamic impact forces experienced by structures due to failed components.” (Tucker, 2007)

3. Modeling supporting towers and transmission line

The electric transmission lines are constructed using different types of supporting structures, viz., (i) Self-supported steel lattice towers,(ii) Guyed V–type steel lattice towers (iii) H-frame wood pole structures (iv) Wood pole structures and (v) Steel tubular structures etc.

In the present research work, in order to determine steady peak dynamic longitudinal loading on the towers, due to sudden conductor rupture, Guyed V- type steel lattice tower was chosen as supporting structures to model a transmission line. The same transmission line model was also used to study collapse of towers due to sudden rupture of conductors in one typical span. The following sub-section describes the modeling of Guyed-V-type steel lattice supporting structure and transmission line model.

3.1 Modeling of Guyed-V Steel Lattice Tower

The Guyed-V steel lattice tower (230kV steel structure) design drawings were provided by Newfoundland and Labrador Hydro. The tower was originally designed for a span of 428m to provide an adequate ground clearance of under a 25mm radial ice load. The tower considered for this analysis is a basic tower with two 6.09 m (20 ft) and 4.752 m (15 ft) extensions.

The Guyed-V steel lattice tower consists of four main components-

- Lower mast
- Top mast

- Cross-arm
- Mast extensions

The elevation view of the Guyed-V steel lattice tower is shown in Figure 3.1

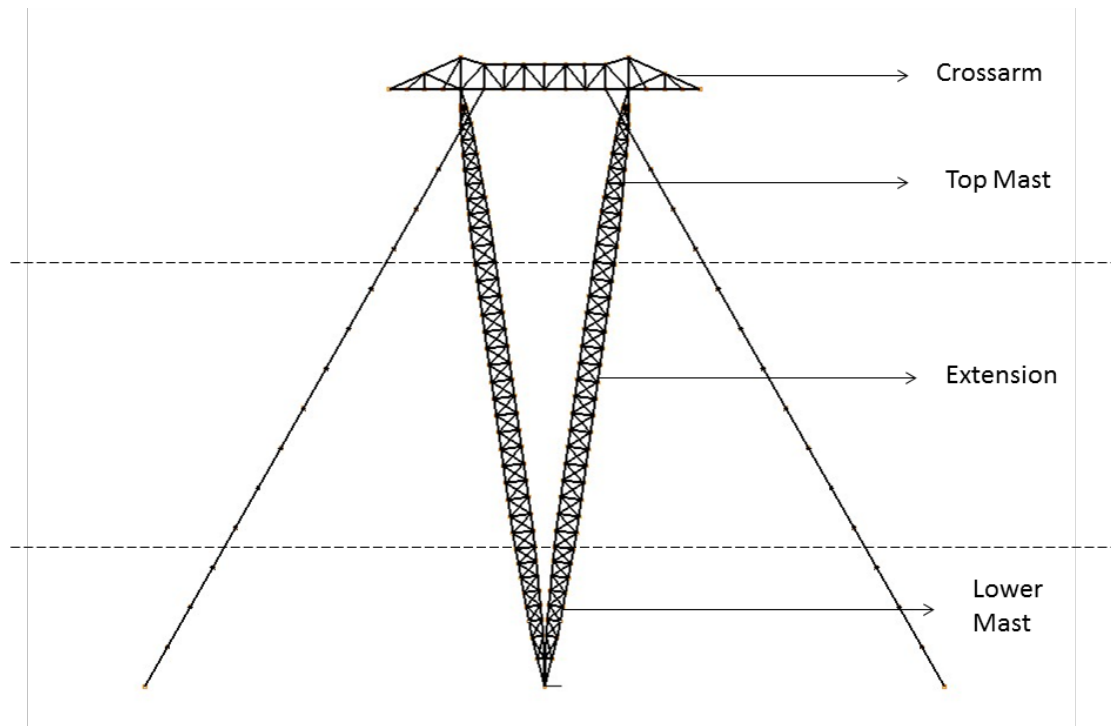
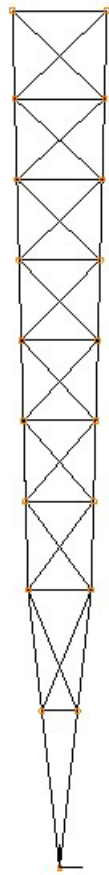


Figure 3.1 Elevation view of Guyed-V Steel Lattice Tower

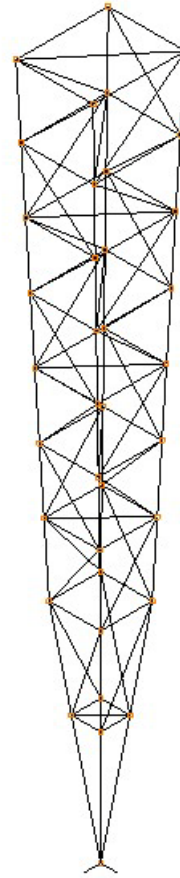
The structural members of the Guyed-V steel structure consist of several types of L-sections. Typically, the main columns of masts and main elements of the cross-arm comprised of L64 x 64 x 4.8 mm sections. The brace elements used different L-sections; L44 x 44 x 3.2 mm, L51 x 51 x 3.2 mm and L44 x 44 x 4.8 mm.

In order to develop the finite element models, one needs to know the geometrical three dimensional coordinates of the points where the members connect along with the member

connectivity, and the type of the section. To facilitate this, a geometrical model of each component was generated using AutoCAD, using the physical dimensions from the design drawings. From these geometrical models, the coordinates of points and member connections, where each member got connected, was extracted. The type of section used corresponding to each member was extracted from the design drawings.



Elevation View of Bottom Mast of
Guyed -V Steel Lattice Tower

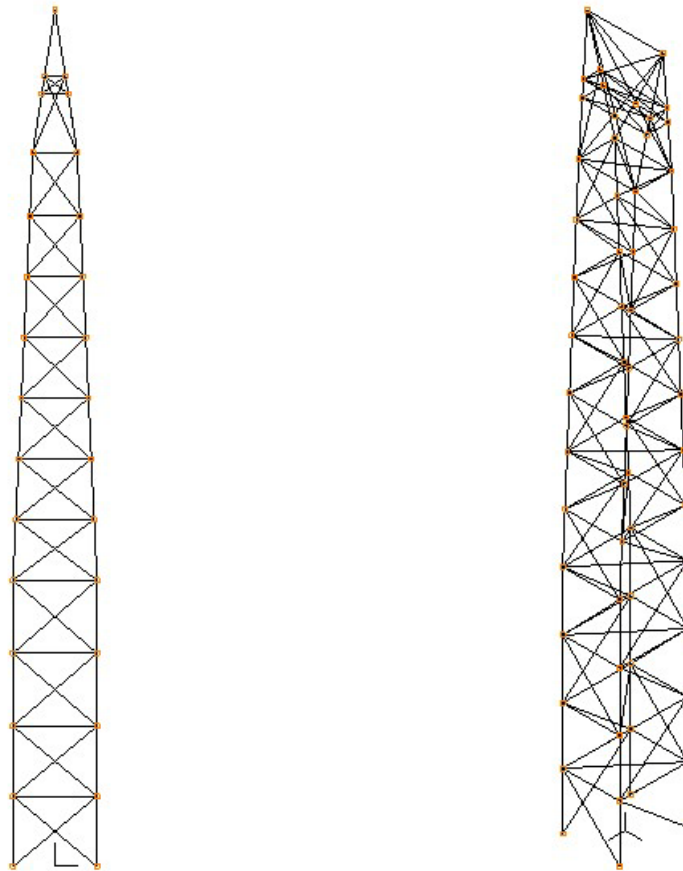


Isometric View of Bottom Mast of
Guyed -V Steel Lattice Tower

Figure 3.2 Bottom Mast Guyed-V Steel Lattice Tower

The geometrical model of the lower mast is shown in Figure 3.2. The columns of the lower mast were single members of the L-section and the cross bracing members were connected to the main column by bolts. The cross-bracings were of L44 x 44 x 3.2 mm cross-section, while the columns belonged to the section L64 x 64 x 4.8 mm.

The geometrical model of the top mast is shown in Figure 3.3



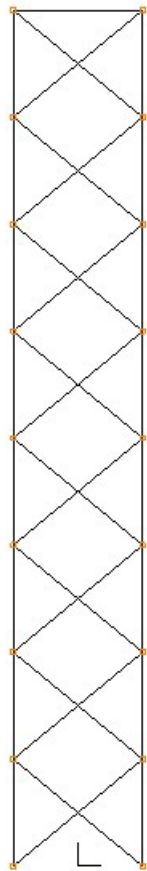
Elevation View of Top Mast of
Guyed -V Steel Lattice Tower

Isometric View of Top Mast of
Guyed -V Steel Lattice Tower

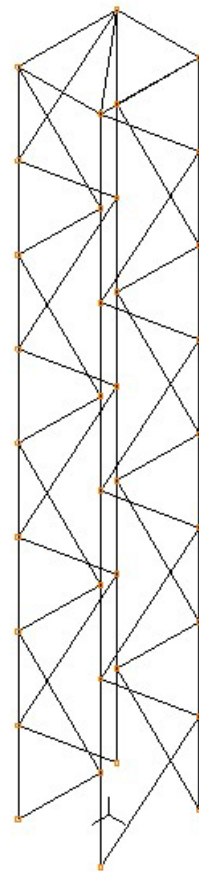
Figure 3.3 Top Mast of Guyed-V Steel Lattice Tower

Similar to the lower mast, the cross bracings were connected to the top-mast's columns by bolts. The cross-bracings and the columns were of L44 x 44 x 3.2 mm and L 64 x 64 x 4.8 mm sections respectively.

Figures 3.4 and Figure 3.5 show the elevation and isometric views of the extension masts. The cross-sections of the columns and cross-bracing members in these extension masts were the same as in lower and top masts.

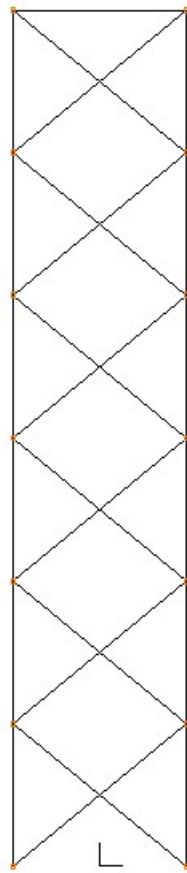


Elevation View of 6.09 m (20 ft)
Extension of Guyed V-type Steel Lattice
Tower

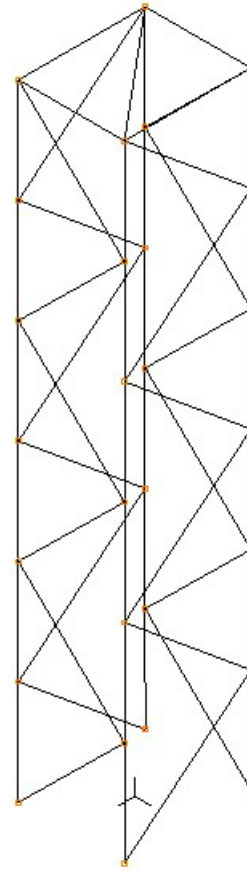


Isometric View of 6.09 m (20ft.)
extension of Guyed V Steel
Lattice Tower

Figure 3.4 Extension 26.09 m (20 ft.) of the Guyed-V Steel Lattice Tower

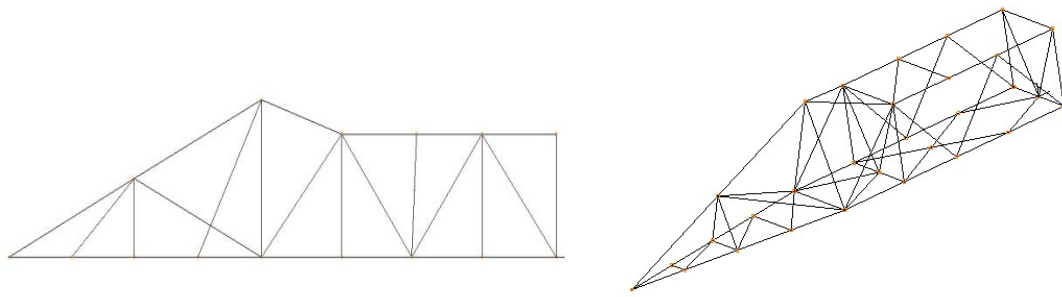


Elevation View of 4.57 m (15 ft)
Extension of Guyed V-type Steel Lattice
Tower



Elevation View of 4.57 m (15 ft)
Extension of Guyed V-type Steel Lattice
Tower

Figure 3.5 Extensions 15 feet of the Guyed-V Steel Lattice Tower



Elevation View of Cross-arm of
Guyed-V Steel Lattice Tower

Isometric View of Cross-arm of
Guyed-V Steel Lattice Tower

Figure 3.6 Half Cross-arm of the Guyed-V Steel Lattice Tower

The geometric model of the one-half of cross-arm is illustrated in Figure 3.6. The main members of the cross-arm were continuous members with L64 x 64 x 4.8 mm, L76 x 76 x 4.8 mm and L76 x 51 x 6.4 mm sections. Other members, apart from the bracings, belonged to sections L76 x 76 x 6.4 mm, L51 x 51 x 4.8 mm and L64 x 51 x 4.8 mm. It was seen from the design drawings that all the cross brace members were connected to continuous columns with bolts. Therefore, the connections of the cross brace members with the column were neither pinned nor rigid connections, they were semi-rigid connections.

After generating the coordinates of connection points and member connections, a geometrical model of a single mast was developed, treating the mast to be standing in a vertical position. This was achieved by placing the mast extensions on top of the lower mast and the top mast was placed over the extension. The geometrical model of the single mast in vertical position is shown in Figure 3.7.



Elevation View of Vertical Mast of
Guyed-V Steel Lattice Tower



Isometric View of Vertical Mast of
Guyed-V Steel Lattice Tower

Figure 3.7 Vertical Mast of the Guyed-V Steel Lattice Tower

From the position where top mast was connected to the cross arm (see Figure 3.8), the inclination of the mast with the vertical line from the base support was determined. Using this inclination (or angle), the coordinates of the connection points of members were transformed to provide the coordinates in reference coordinate axes X, Y and Z, where Y-axis was in transverse direction (perpendicular to the plane of the tower). Using the symmetry of the tower, about X-Y plane, passing through the support point, the

coordinates of the points, the member connections and the type of member sections were generated.

The four guy-wires were connected to the cross-arm at a particular distance from the symmetric section and the ground with predetermined angles. Therefore, using these end points, the guy-wire geometry was developed. The full geometric model of Guyed-V steel lattice tower is shown in Figure 3.9.

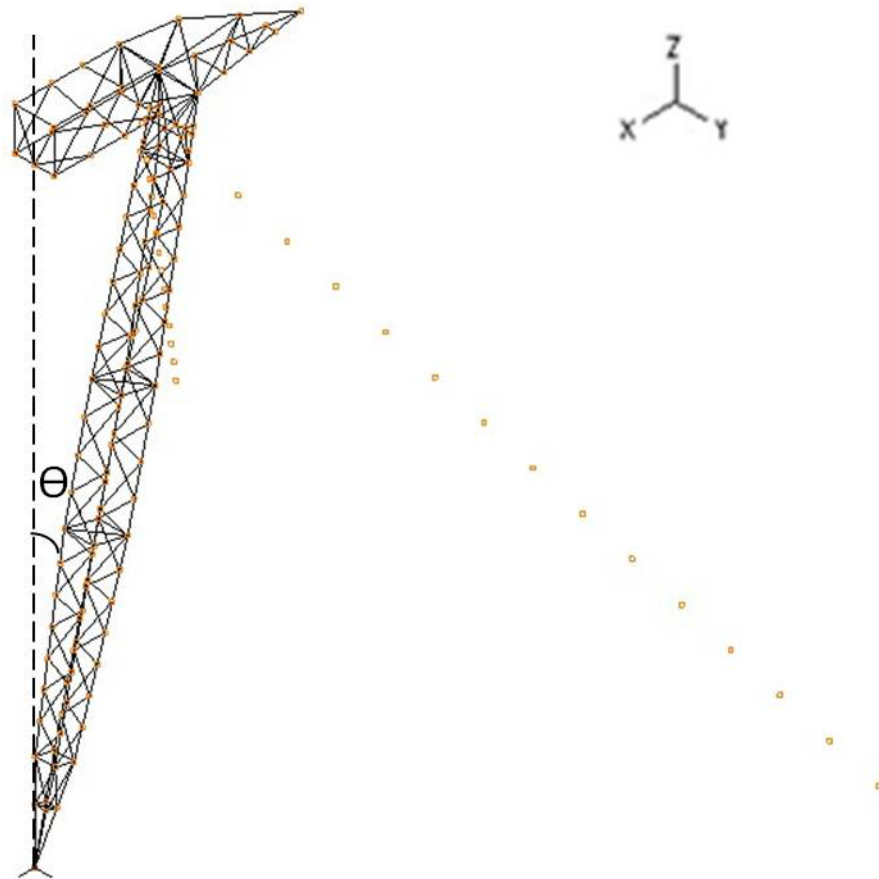


Figure 3.8 Symmetric Half of the Guyed-V Steel lattice Tower



Figure 3.9 Geometrical Guyed-V Tower (Isometric View)

3.2 Modeling of Supporting Tower Members

It is common practices to model supporting steel lattice towers based on the assumption that all its structural members, viz., continuous columns, cross-arm members and cross brace members behave as truss members. Therefore, the numerical analysis of these transmission towers is generally conducted assuming all the members act as truss members and considering that each joint is pinned (or hinged). This assumption may lead to a few discrepancies.

In a real tower, the main columns and bridge members are continuous angle sections and cross members are connected by bolts. The connection between main structure elements and cross braces are neither completely pinned connections, nor completely rigid connections. Due to this reason, even the joints are not completely pinned connections. In fact, majority of tower constructors rely on full scale tests to ascertain the safety of these towers.

Murty K. S. Madugula *et al.* (1998) modelled a Guy mast as a truss element and later as a beam element and compared the results. The natural frequencies obtained from both the models were observed to be almost similar to one another.

J. G. S da Silva *et al.* (2005) proposed an alternative structural analysis modelling strategy for steel tower design. The model combined the three-dimensional beam and truss elements to account for the structural forces and bending moments. The results obtained in this experiment showed that the frequency values of the towers considered remain almost the same in all the three models. However, it is proven that the designing of the truss element model is more time consuming and elaborate, due to the necessity of adding dummy bars or elements.

Marcel Oliveira *et al.* (2007) discussed the various problems associated with the traditional approach of considering tower members as truss elements. This paper proposed the alternative method of structural analysis, where the modelling strategy involved the use of a mixed element approach, where the members of the tower were considered as truss and beam elements. They performed static, dynamic, stability and

non-linear analysis to show the advantages of adopting beam element members in the tower design. The conclusions were drawn after carefully studying and comparing the data obtained from individual analysis of different model strategies. They also showed the limitations in some sections of the tower, where the members did not show much variation in the results when they were changed from truss to beam elements.

Therefore, in order to determine the natural frequencies of the tower and transmission line, the tower structures were modeled using the following approaches.

- **Truss Model:** All the structural members were modeled as three dimensional truss members with linear elastic material property. The connections of members were assumed to be pinned connections. Therefore, each node of the structure had three degrees of freedom (translational displacement), in X, Y and Z coordinate directions only.
- **Beam Model:** All the structural members were assumed as beam elements with linear elastic material properties. The joints were considered to be rigid joints with six degrees of freedom, namely three translational displacements and three rotational.

3.3 Conductor Modeling

Three conductors were modeled using three dimensional nonlinear elastic truss elements, with initial conductor tension of twenty percent of the rated tensile strength of the material. These conductors were strung between the towers, as shown in figure 3.9. ACSR (Aluminum Conductor Steel Reinforced) 795 Conductor (trade name- DRAKE)

(Munaswamy and Haldar, 1997) was chosen for this investigation. The various characteristics considered in modeling the conductors for this analogy can be seen in Table 3.1.

Table 3.1 Conductor Characteristics of the Transmission Line

Conductor Characteristic	Characteristic Value
Type of the Conductor	ACSR 795
Trade Name	DRAKE
Number of Aluminum layers	2
Initial Conductor Tension	27.8kN
Area of Aluminum	0.0004028 m ²
Area of Steel	0.0000656 m ²
Total Cross-sectional Area	0.000468 m ²
Core Diameter	0.02813 m
Mass	1623 kg/km
Rated Tensile Strength	139 kN

The conductors strung between any two towers were divided with thirty elements. Using the end points of the conductor, in each span, the nodal coordinates were produced. Each end of the conductor, in each of these spans, was connected to the insulator strings, using catenary equations.

Both the conductor and guy-wires were modeled as an assembly of tension-only truss elements. Hence, modulus of elasticity was zero for compressive axial strains and modulus of elasticity was stipulated for tensile axial strains.

The appropriate input file format, for ADINA, was generated with the help of a JAVA program. The data essential for the generation of transmission line system included the nodal point-coordinates, line and element connectivity data, element cross-sectional area information, weight density, modulus of elasticity, conductor properties (as mentioned in Table 3.1) and conductor attachment points with the insulator string, with respect to the origin of tower coordinate system and insulator string length. Also, the data pertaining to the foundation coordinates for each tower location, with respect to the first tower was provided in the input file. According to this data, the X and Y coordinates dictated the transverse and longitudinal direction of the line respectively while the Z coordinates described the elevation of tower foundation.

Using all the above data, a transmission line system, comprising of thirty-one tower structures, was generated. The generated finite element model is shown in Figure 3.10

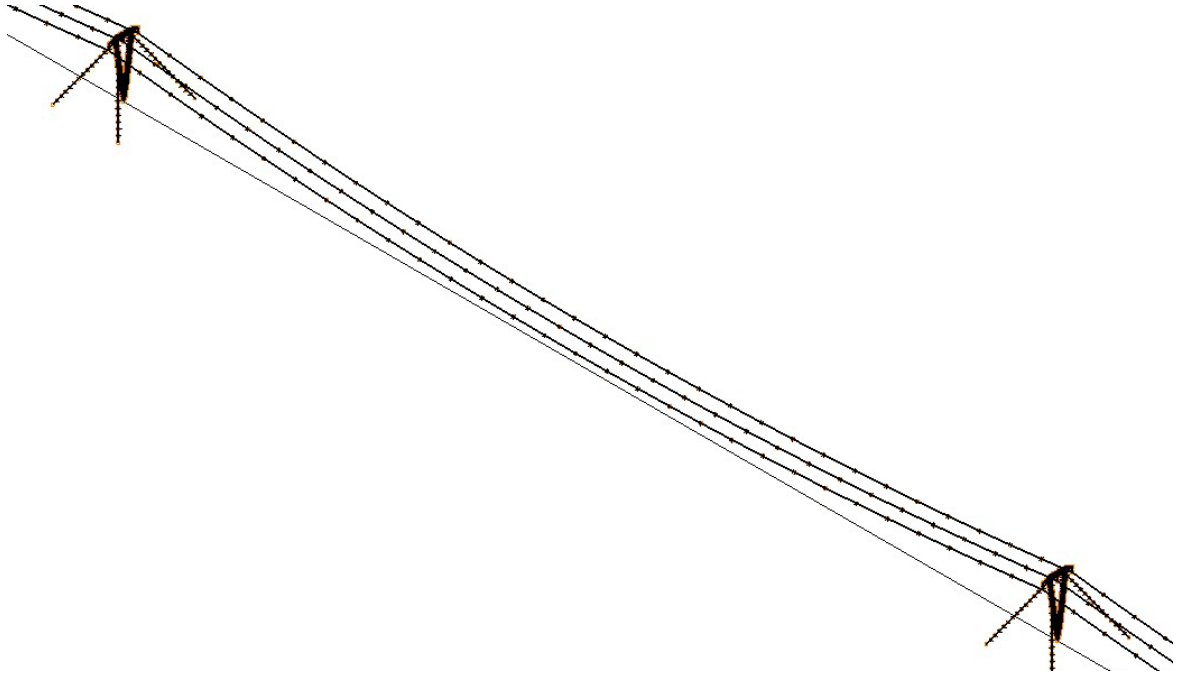


Figure 3.10 Section of the Finite Element Model of the Transmission Line Model

4. Free Vibration Analysis and Damping

In order to determine the maximum dynamic forces experienced by the tower due to sudden rupture of conductors in any span, using explicit or implicit transient dynamic analysis procedure, one needs to consider damping in the tower conductor. Generally, the damping in the towers and conductors are not the same. Damping in the tower may be greater than damping in the conductors. Rayleigh damping is often used in the dynamic analysis. Before using Rayleigh damping, the natural frequencies of tower and transmission line were determined. The following subsections describe the free vibration analysis of tower and transmission line.

4.1 Free Vibration Analysis of Tower

The free vibration analysis was conducted to find out the natural frequency of the tower for both, truss and beam models of the tower. Figure 4.1 to Figure 4.3 depict the corresponding bending and twisting mode shapes for the first three significant frequencies of both the truss and beam models. This analysis is necessary, because when the frequency of the tower (or line), under excitation loading conditions, reaches the natural frequency of the tower (or line), the structure would collapse.

Table 4.1 Frequencies of Significant Twisting and Bending Modes in the Towers

Frequency Mode	Type of Mode	Frequency (rad/s) Tower Modeled using truss elements	Frequency (rad/s) Tower Modeled using truss elements
1	Twisting	12.93	13.09
2	Bending	14.25	14.38
3	Twisting	24.57	25.47
4	Bending	26.57	27.39
5	Twisting	46.312	48.60

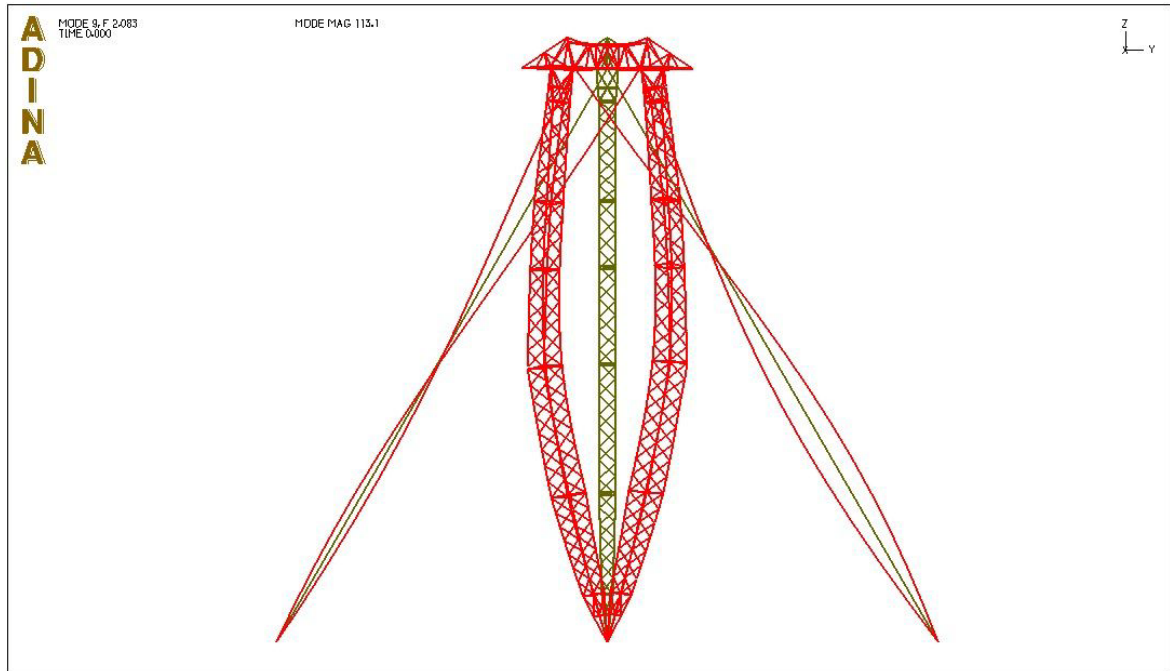


Figure 4.1 Mode 1 of the Transmission Tower

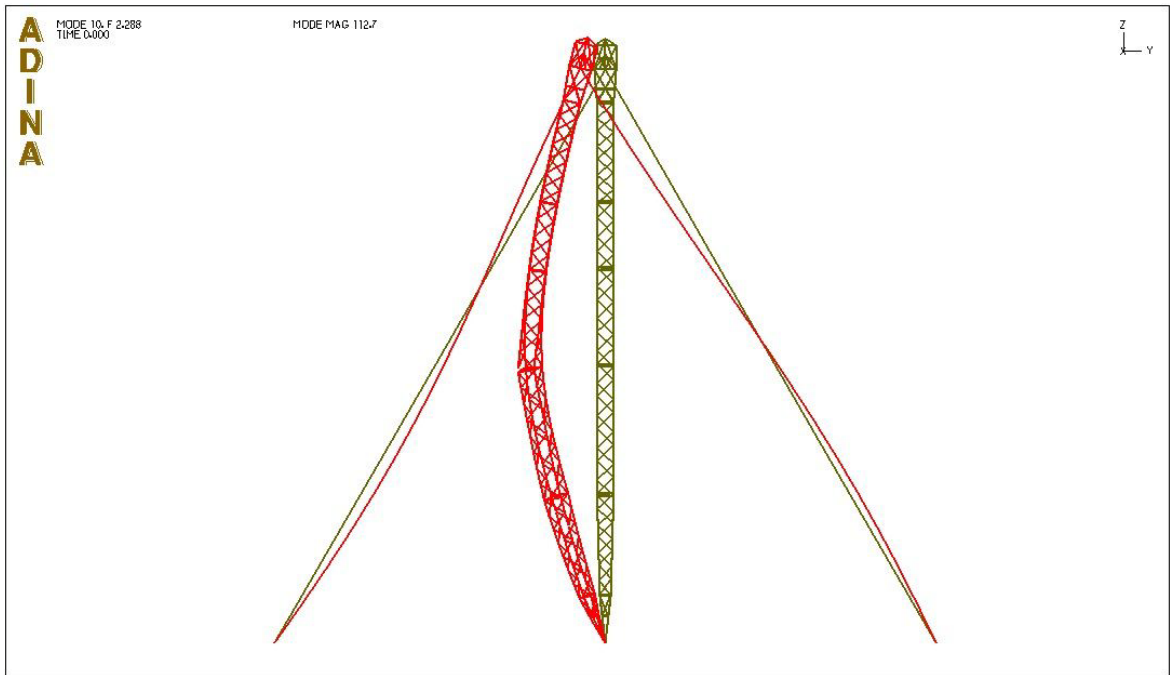


Figure 4.2 Mode 2 of the Transmission Tower

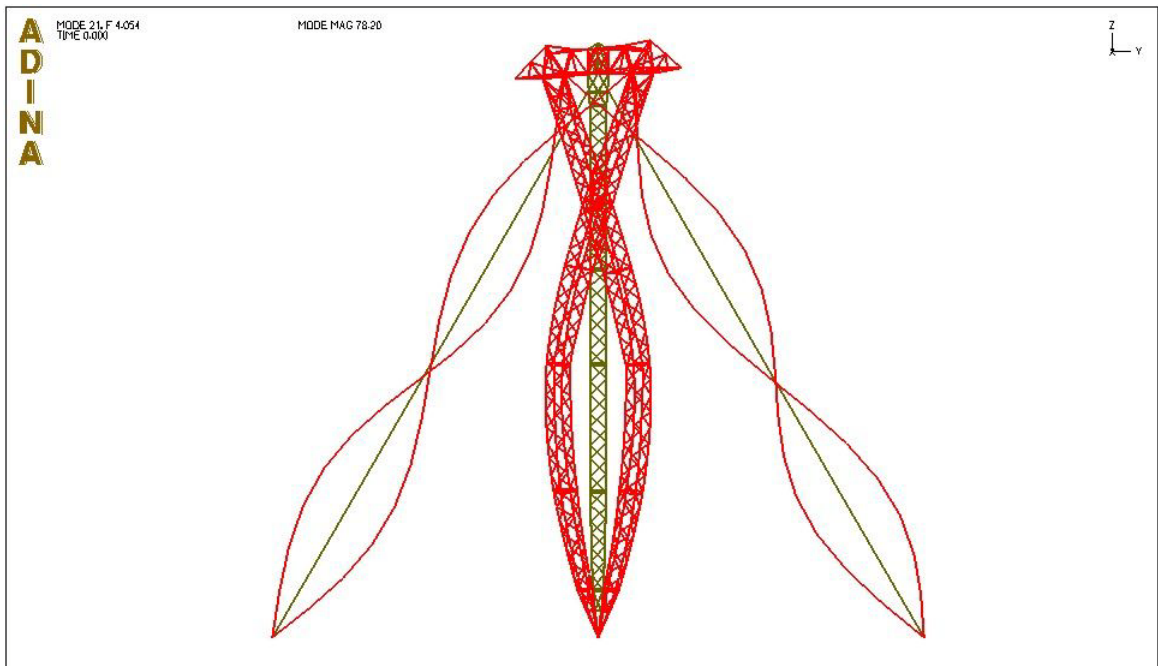


Figure 4.3 Mode 3 of the Transmission Tower

After examining the natural frequencies of both models, it was observed that the numerical values of natural frequencies were slightly larger for beam model, when compared to the truss model. Also, was noted that the mode shapes for both models are the same.

4.2 Free Vibration Analysis of Transmission Line

Free vibration analysis of transmission line model generated with supporting structure using truss elements and beam elements was conducted to obtain the natural frequencies and mode shapes since only the vibration modes, corresponding heave modes, participate in the transient dynamic analysis. These modes were identified by examining the mode shapes. The natural frequencies of heave mode shapes are presented in Table 4.2. These natural frequencies, associated with the heave mode, were within the expected range. Mode shapes, corresponding to these modes, are shown in Figure 4.4 to Figure 4.6.

Table 4.2 Natural Frequencies of Transmission Line Systems

Frequency Mode	Frequency of line with Truss model (rad/s)	Frequency of line with beam model (rad/s)
1	0.3748	0.3748
2	0.6291	0.6291
3	0.7665	0.7665

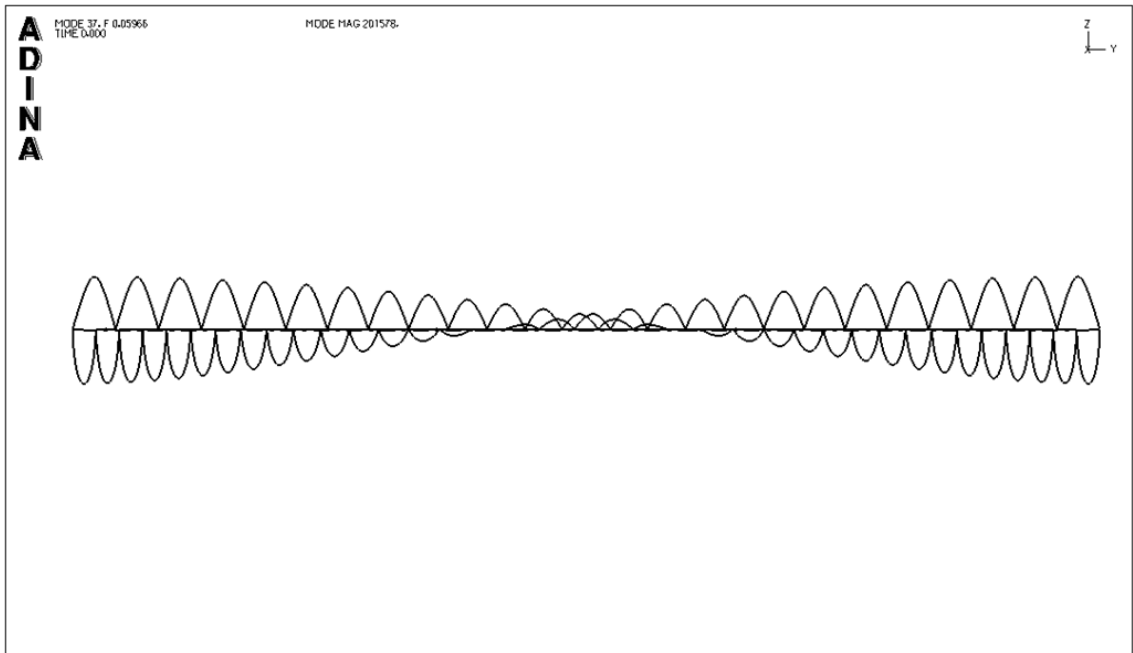


Figure 4.4 Mode 1 of the Transmission Line

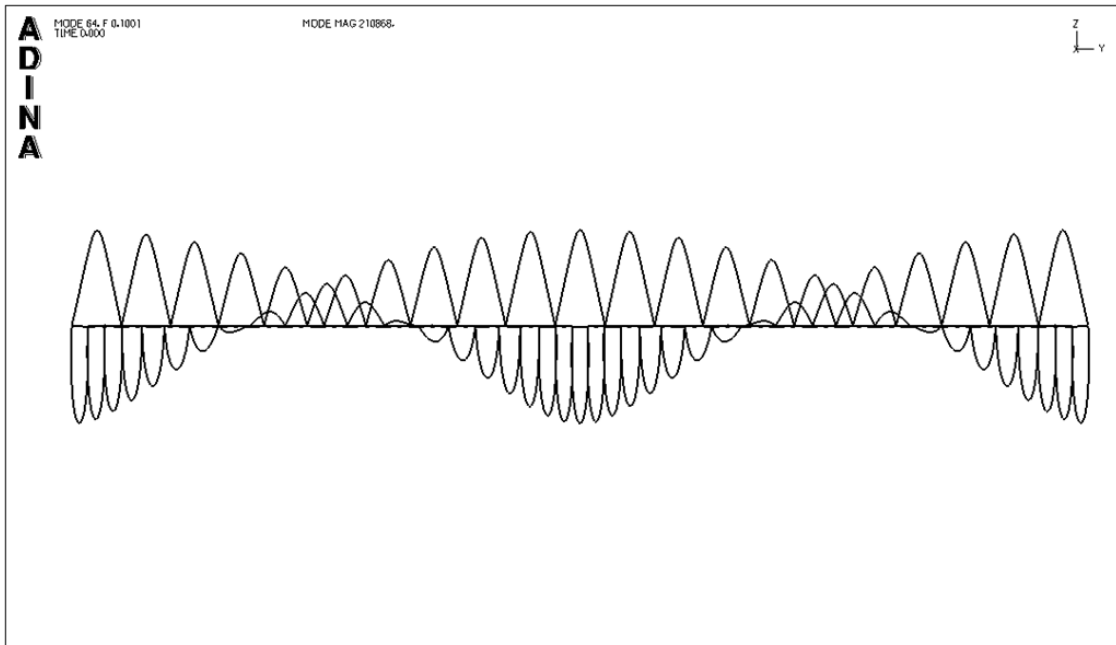


Figure 4.5 Mode 2 of the Transmission Line

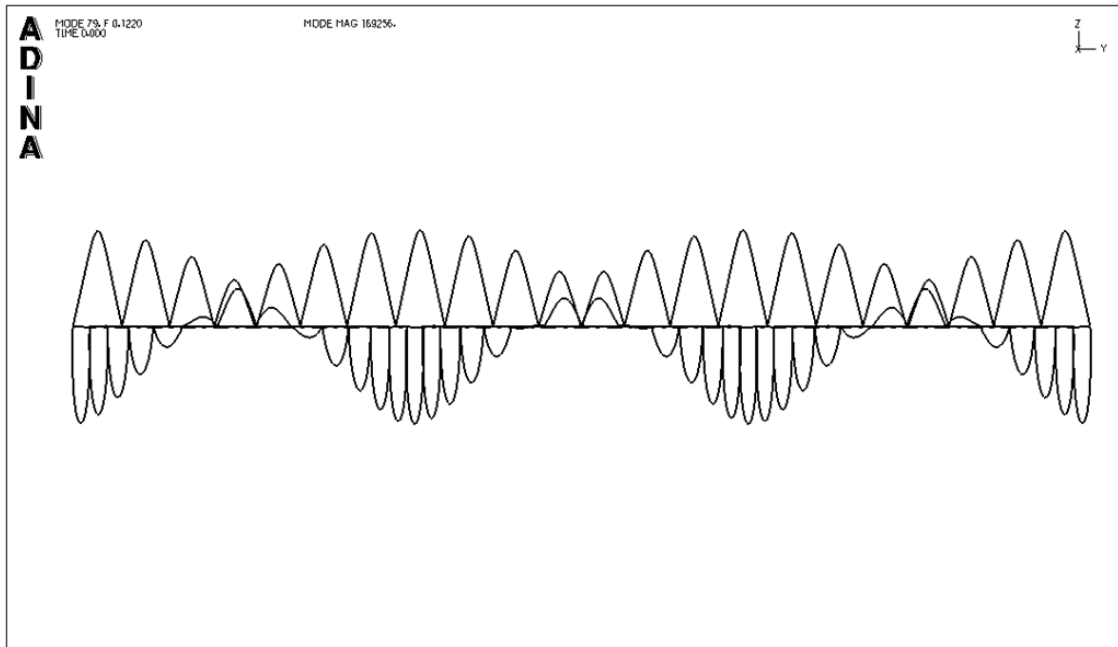


Figure 4.6 Mode 3 of the Transmission Line

It can be observed that the natural frequencies of the transmission line do not depend on the type of supporting structures of transmission line, but only depend on the initial tension of the conductors.

4.3 Damping

Damping is essential for the transient analysis of line due to broken conductor, because un-damped systems may not provide correct results. Therefore, for this study Rayleigh damping was used.

The Rayleigh damping coefficients were used in conjunction with mass and stiffness matrices to determine the damping matrix. The damping matrix is given by-

$$[C] = \alpha[M] + \beta[K] \quad 4.1$$

Where,

α and β are the Rayleigh damping coefficients,

$[M]$ is the total system mass matrix and

$[K]$ is the stiffness matrix

The critical damping ratio ξ_i for mode 'i' is given in terms of Rayleigh damping coefficients as-

$$\xi_i = \frac{\alpha}{2\omega_i} + \frac{\beta\omega_i}{2} \quad 4.2$$

Where, ω_i is the natural frequency of the system, for the i^{th} mode of vibration.

In this present analysis, a damping matrix proportional to mass matrix was considered, as only mass-proportional Rayleigh damping is available in explicit analysis (ADINA, 2003), therefore there was little damping for the higher modes of the structure. Hence, the value of β was taken as zero. The Rayleigh damping constant, α , was calculated using the equation 4.2. From the equation, it was clear that the damping matrix had elements in the diagonal only.

The value of ξ_i was taken as 0.02 for the transmission line conductors, whereas it was considered to be 0.05 for the transmission towers. The values of the damping ratio were calculated using the natural frequencies of the two element groups, in order to build the

damping matrix. Hence, the Rayleigh coefficient, α , was found to be 0.015 for the transmission line and 1.37 for the transmission tower.

5. Static and Transient Dynamic Analysis of Transmission Line with Broken Conductor

The static and dynamic analyses were carried out over the transmission line models viz., truss model support structure line system and beam model support structure line system. The primary objective of this analysis was to determine maximum longitudinal loading on the towers adjacent to the span, where the conductors were ruptured. The studies were conducted for two cases viz., a) Transmission line with bare conductor (i.e. no ice on the conductor) and b) Transmission line with 25mm (1-inch) radial ice on the conductor. The following subsections will outline the procedure used for conducting these static and dynamic analyses.

5.1 Initial Static Analysis

Static analysis is generally conducted to bring the transmission line model into static equilibrium condition under gravity loading. During the static structural analysis, inertial effects or damping criteria are not considered. This analysis is performed to determine forces (or displacements, stresses and strains) in particular components or nodes or elements in the structure under the influence of the gravity load.

A large displacement non-linear static analysis, with mass proportional loading, was performed in this study. Mass proportional loading simulate gravity loading on the conductor and supporting structures. This static analysis was required to bring the finite element model to a static equilibrium.

The results obtained from this static analysis were stored in a file, and later used in subsequent transient dynamic analyses. The restart file comprised of the data, necessary for the restart analysis, like the element deformations, system configuration, stress-strain data etc. The restart data was saved only at the end of static analysis.

The initial tension in the insulator strings and the conductors were extracted from the static analysis. The tensions in the conductors were very close to the initial tensions (27.87kN) used in generating the finite element model for the conductors and the tensions in the insulator strings were equal to the weight of the conductor between spans (6.92KN)

5.2 Broken Conductor Transient Dynamic Analysis

Conductors were modeled using catenary equation using self weight of the conductor and initial tension. Conductors on each side of the insulator string, to which the conductors are attached, were under the same initial tensile load. The insulator (in static equilibrium) experienced only the gravity loads of the conductor, since tension on either side of the insulator was balanced. A small section of the transmission line, under static equilibrium, is illustrated in Figure 5.1 below.

But, when the conductors in a span were ruptured, due to the sudden release of tension, the loads got redistributed to the insulator strings adjacent to that span, where conductor breakage was simulated. Therefore, it was seen that the insulators swing away from their static equilibrium vertical position (see Figure 5.2) under the influence of this dynamic load. Peyrot, Kluge and Lee (1980) suggested that when a conductor break occurs in a span, the initial strain energy stored in the conductors is suddenly released, which causes

the insulator and the conductor in the adjacent span to move away from the span, where conductor breakage occurs. Immediately following the rupture of the conductor, the insulator string swings, as a rigid body, along with the conductor and the tension in the insulator reduces to almost zero and later, as the conductor falls back, the tension in the insulator increases. They presented a force history at the insulator assembly, after conductor rupture, which is illustrated in Figure 5.3.

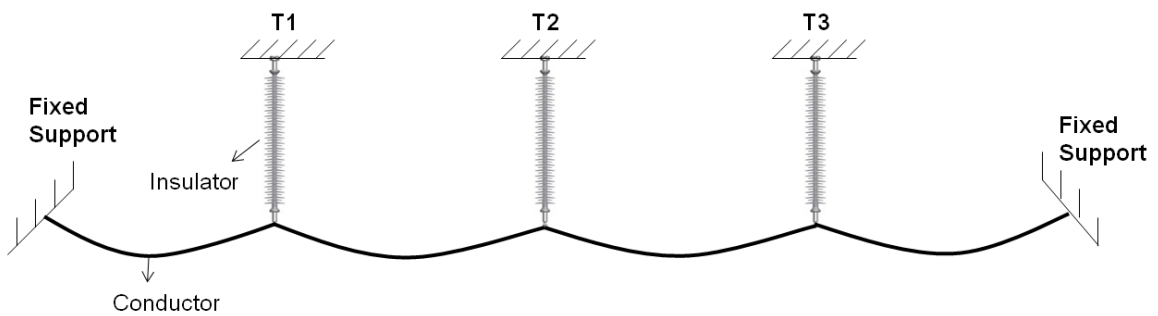


Figure 5.1 Transmission Line Section in Static Equilibrium

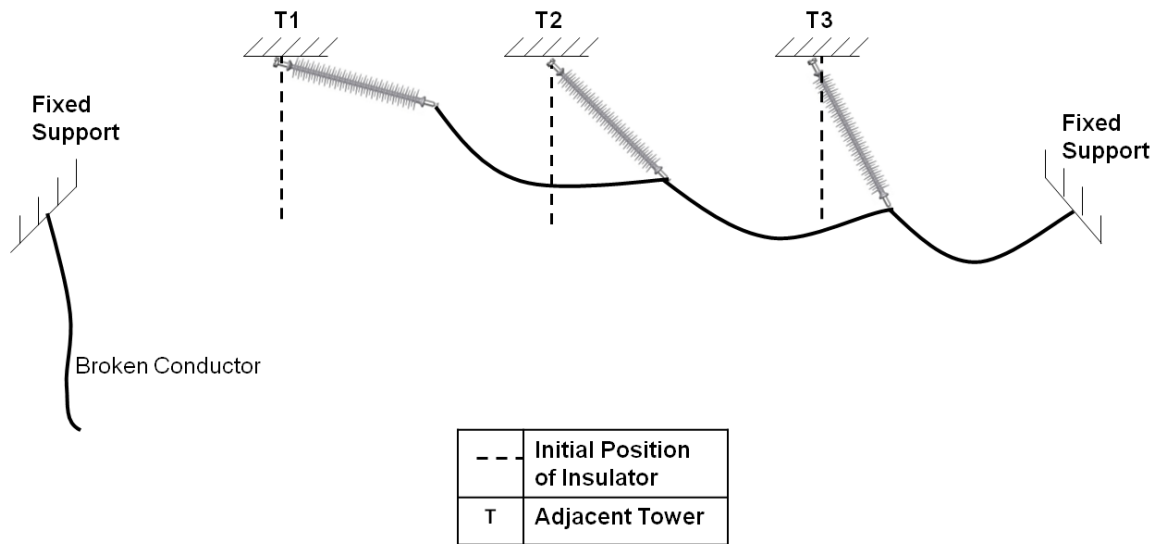


Figure 5.2 Transmission Line Section after Conductor Rupture in one of the Span

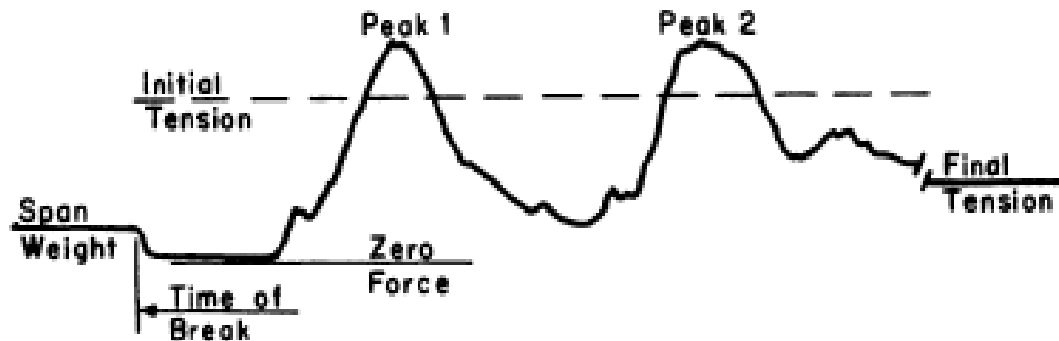


Figure 5.3 Force in the Insulator after Broken Conductor (Peyrot, Kluge and Lee, 1980)

In the present study, the transient dynamic analysis was conducted to determine the dynamic tensions in the insulator strings and thereby the longitudinal loads on the supporting towers due to conductors' rupture from the static equilibrium state of the line model. The conductor rupture was simulated by using the death element option in ADINA and the time of rupture was set to 1.001 second (after static analysis). When

death element option is used, the element will be removed from the model and no stiffness and mass matrices are added to the system matrices.

The dynamic analysis was carried out using the restart option and the method implemented to perform this test was explicit direct integration method. Properties like damping, material weight density, time steps etc. were manually changed in the data input file before conducting the dynamic analysis. However, parameters like the line configuration data and cross-sectional properties of the elements in the transmission line system must not be changed

The time history of insulator tension for the insulators on the two towers adjacent to the conductor rupture, for both the truss and beam models, is presented in Figure 5.1 and Figure 5.2. From the time history data, maximum dynamic tensions in insulator strings on adjacent towers were extracted and presented in Table 5.1.

It can be observed that the sudden rupture of conductors caused the insulator strings in the adjacent towers to experience an unbalanced tension. The insulator strings in first tower adjacent to the conductor breakage have been observed to experience the maximum dynamic forces, in both the models. Also, it can be noted that the forces in the subsequent tower decreases, as we move away from the conductor rupture.

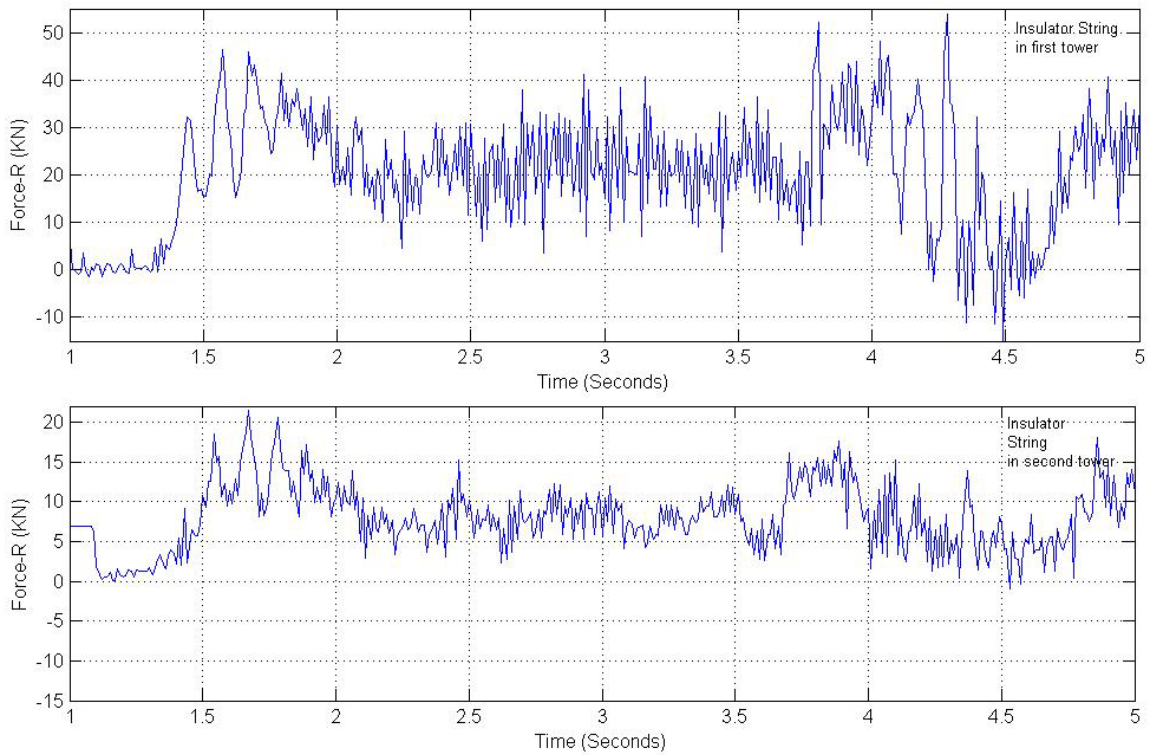


Figure 5.4 Time History of Insulator Tension for the Insulators of Adjacent Towers to Conductor Rupture in Truss Model

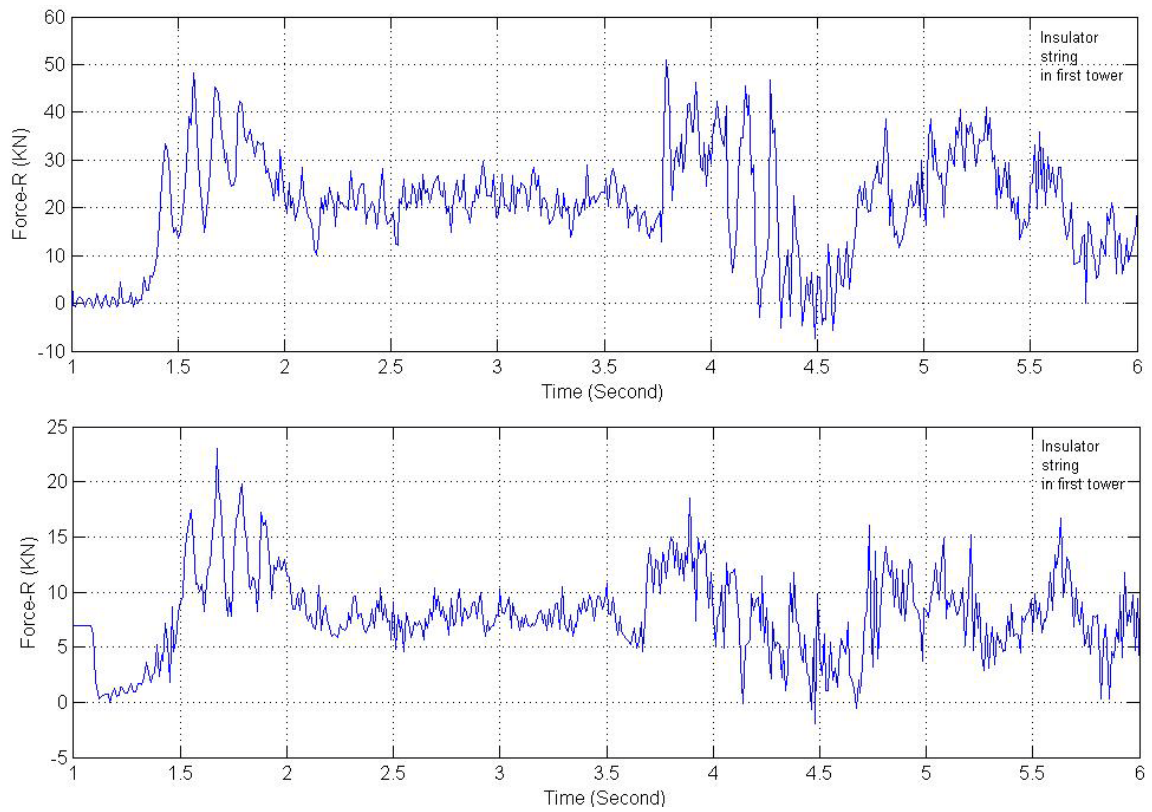


Figure 5.5 Time History of Insulator Tension for the Insulators of Adjacent Towers to Conductor Rupture in Beam Model

Table 5.1 Maximum Dynamic Tensions in Insulator Strings on Adjacent Towers

Insulator string	Maximum dynamic tension in Truss Line Model (kN)	Maximum dynamic tension in Beam Line Model (kN)
Insulator string in 1 st tower adjacent to conductor break	45.40	48.32
Insulator string in 2 nd tower adjacent to conductor break	20.88	22.99
Insulator string in 3 rd tower adjacent to conductor break	17.33	17.80
Insulator string in 4 th tower adjacent to conductor break	15.89	15.49
Insulator string in 5 th tower adjacent to conductor break	14.82	15.13

5.3 Transient Dynamic Analysis for Ice-Loaded Conductor when Conductors are Ruptured

5.3.1 Ice Simulation on the Conductors

The ice loading on the conductor was simulated by changing the weight density of the conductor material. After the initial static test, the weight of the conductor was increased from 3,478.5 N/m² to 11,105 N/m². The weight density of the conductor was calculated with the help of conductor cross-sectional area and the mass density of ice.

The diameter of the conductor (D_i) is 28.13 mm, the thickness of the radial ice (t), covering the conductor, is 25.44 mm and the density of ice (ρ_w) is 917 kg/m³. Figure 5.3 gives an illustration of the cross-section of the conductor, with radial ice loading. The total diameter of the cross section, D_o , is given by-

$$D_o = D_i + 2 \times t$$

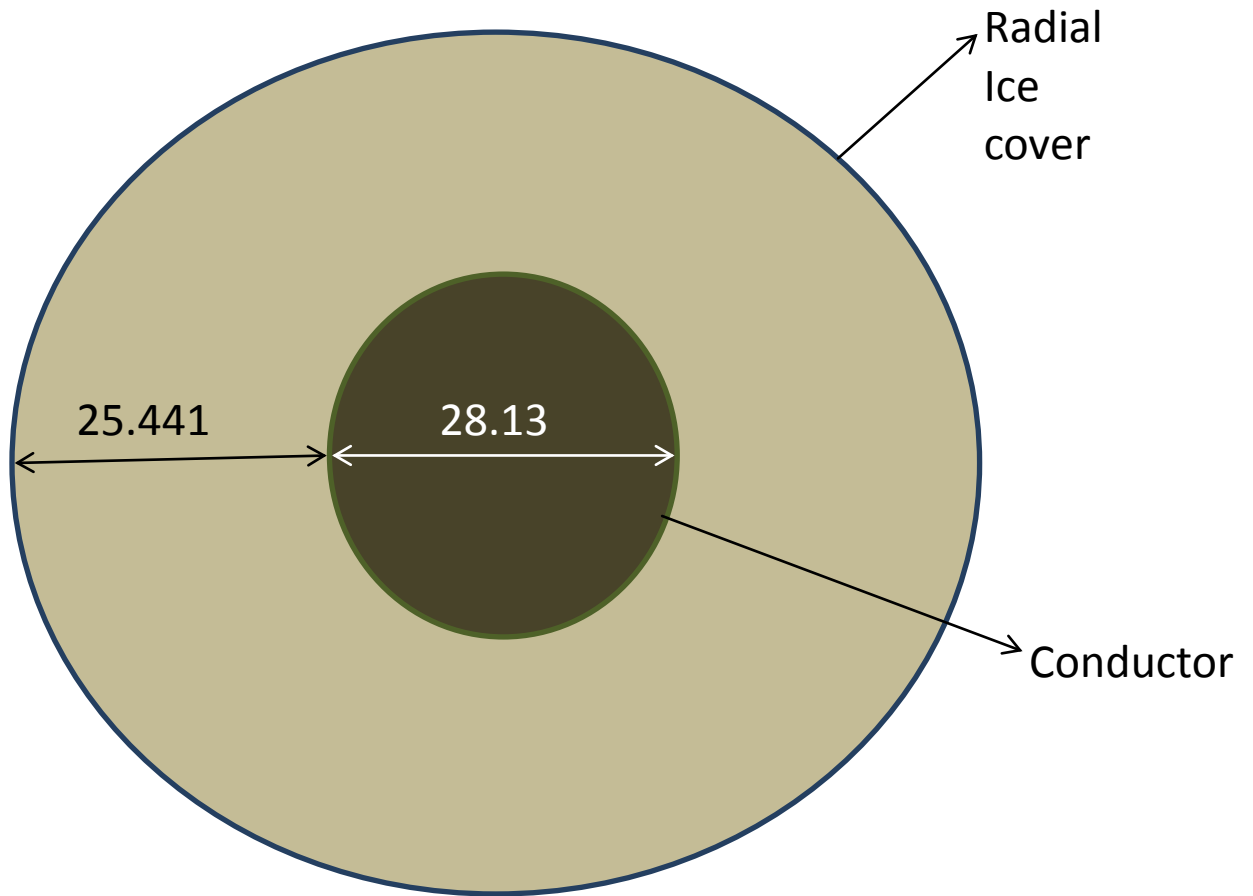


Figure 5.6 Schematic Cross-sectional View of a Loaded Conductor

Therefore, the weight of the ice, W_{ice} can be calculated as follows-

$$W_{ice} = \frac{\pi}{4} (D_o^2 - D_i^2) \rho_w \quad (5.1)$$

Substituting the values in the above equation gives W_{ice} as 38.477 N/m. The total weight (W_{total}) of the conductor is 54.447 N/m. Hence, the density of this entire setup (ρ_{total}) will be-

$$\rho_{total} = \frac{W_{total}}{V_{conductor}} \quad (5.2)$$

where, $V_{conductor}$ is the volume of one meter length of conductor. Therefore, the density of the loaded conductor is 11.105 KN/m^3 .

A second static analysis was performed, by using the restart option from the previous equilibrium state (from the bare conductor test), to bring the line system, with the simulated radial ice load on the conductor, to a new static equilibrium. This restart static analysis holds the changed data, like increased conductor tension, increased sag etc., due to the addition of radial ice loads. The restart data got saved at the end of the static analysis.

By extracting the information from the second static analysis, it is observed that the tension in the conductor has also increased to about 72KN . The increased weight of the conductor, due to radial ice loads, in each span is redistributed to increase the tension in the insulator strings (21.93KN) equal to the new conductor weight in the span.

After the second static analysis, damping parameters were provided to all the elements of the transmission line. Then, by invoking the death element, the conductor elements were set to simulate rupture at 2.001 second.

The time history of insulator tension for the insulators on the two towers adjacent to the conductor rupture is presented in Figure 5.4 and Figure 5.5. From the time history data maximum dynamic tensions in insulator strings on adjacent towers were extracted and presented in Table 5.2.

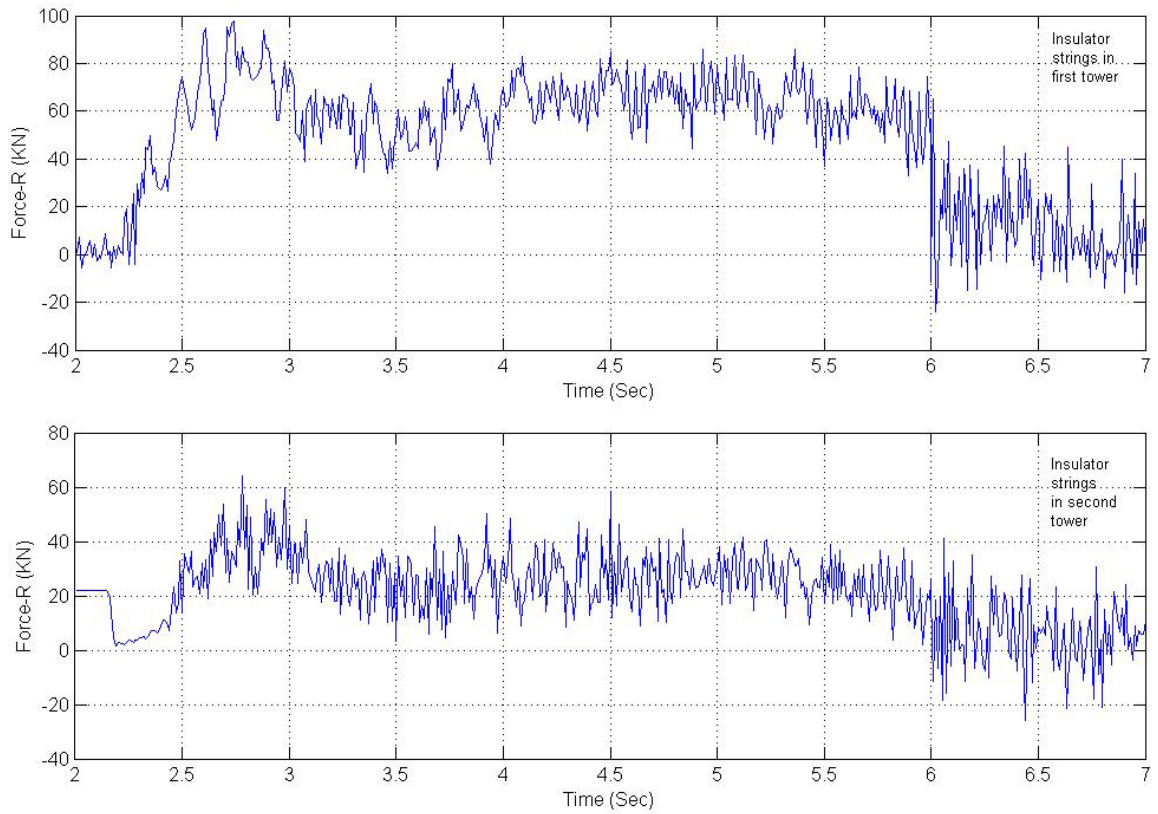


Figure 5.7 Time History of Insulator Tension for the Insulators of Adjacent Towers to Conductor Rupture in Truss Model

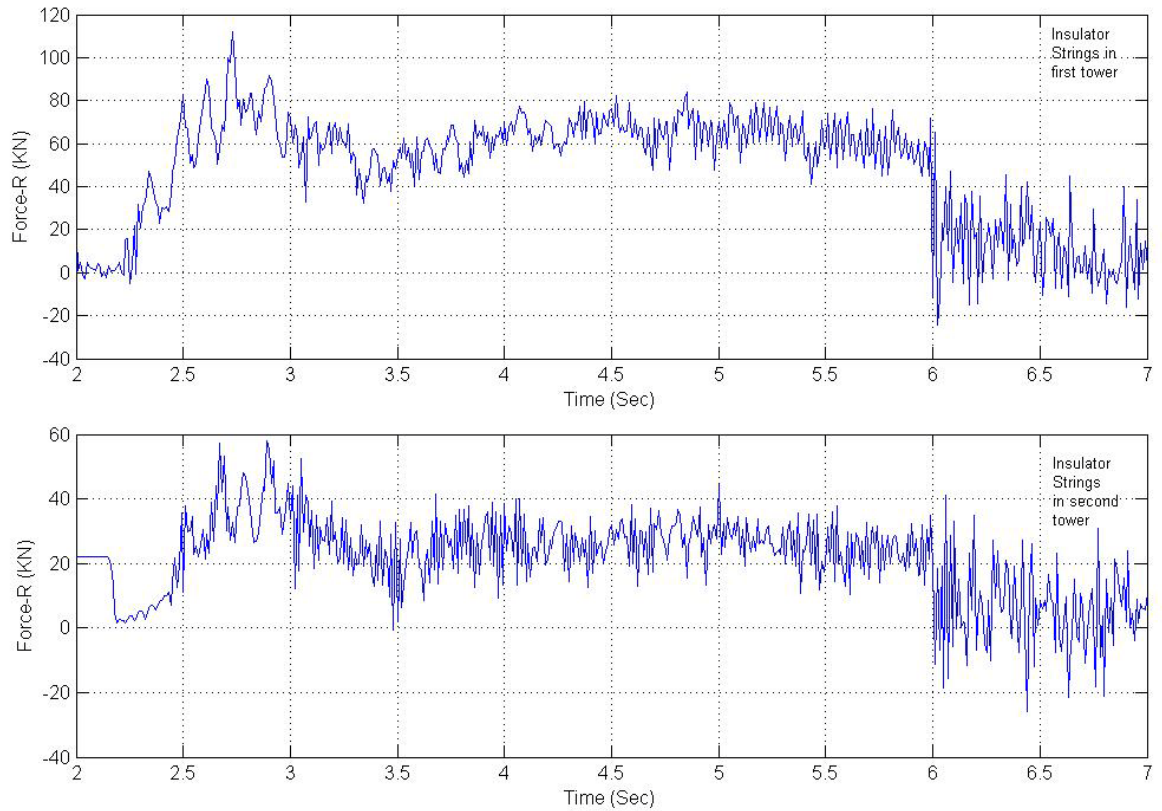


Figure 5.8 Time History of Insulator Tension for the Insulators of Adjacent Towers to Conductor Rupture in Beam Model

Table 5.2 Maximum Dynamic Tensions in Insulator Strings on Adjacent Towers

Insulator string	Maximum dynamic tension in Truss Line Model (kN)	Maximum dynamic tension in Beam Line Model (kN)
Insulator string in 1 st tower adjacent to conductor break	97.73	112.29
Insulator string in 2 nd tower adjacent to conductor break	64.12	57.91
Insulator string in 3 rd tower adjacent to conductor break	43.33	51.59
Insulator string in 4 th tower adjacent to conductor break	40.06	43.85
Insulator string in 5 th tower adjacent to conductor break	36.86	41.61

The above results for broken conductor transient dynamic analysis were obtained by modeling the tower with linear elastic material. With this assumption, the maximum longitudinal loads on the tower are obtained with intact supporting towers (i.e. members in the tower do not fail).

The axial forces and bending moments in the members were examined in order to see whether the stresses in any members were exceeding the yield strength (250MPa) of the members. Figure 5.6 shows two members of the first tower, adjacent to the conductor

breakage, which have been identified to experience a force of about 395.49Mpa for the truss model and 401.85Mpa for the beam model. In fact, they approach the ultimate strength (400 MPa) of the material. The members belong to cross-section L76x76x4.8mm, of the cross-arm bottom column.

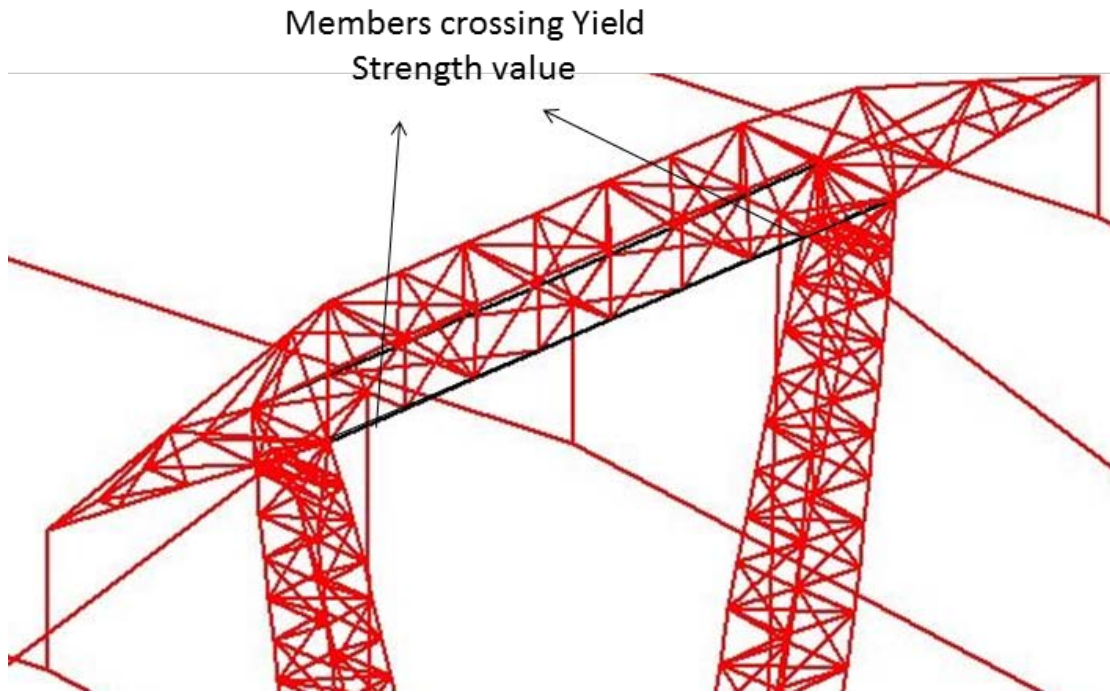


Figure 5.9 Members Identified in the Cross-arm of the First Adjacent Tower

5.4 Closure

After observing the dynamic tensions in the insulator strings from Table 5.1 and Table 5.2, it can be seen that the insulator string tension decreases with increasing distance between the tower and the span where conductor rupture took place. Also, the members, which experience stresses greater than the yield strength of the material, were identified. They are the bridge elements in the cross-arm, as illustrated in Figure 5.9.

The present linear elastic models cannot predict the failure of members or the collapse of the towers. In order to study the collapse of the supporting structures, tower members were modeled using ‘moment-curvature beam’ elements with elastic-plastic material properties. With this model, one can study collapse analysis of supporting structures. The procedure and analysis of this transmission line system, modeled with non-linear material properties, has been presented in the next chapter.

6. Analysis of Moment-Curvature Beam Model

In the previous chapter, the members (truss or beam members) of the supporting structures were modeled using linear elastic material properties. Therefore, failure of members of the supporting structures was not considered. Using this modeling approach, the maximum longitudinal loads of the structures were obtained, due to the rupture of conductors in one of the spans. The member axial forces and bending moments were examined to see whether the stresses in the members were exceeding the yield strength of the material. It was found that some of the main beam members experienced stresses beyond the yield strength value of the material. Since these models cannot be used to predict failure of the members or collapse of the structure, the transmission lines are modeled using Moment-Curvature Beam model using elastic-plastic material properties, which is available in ADINA software.

The moment-curvature plasticity model consists of uni-axial plasticity laws respectively applied to the axial strain, each bending curvature and twist angle per unit length. According to the theoretical manual of ADINA (2003), the element section can be plastic with respect to axial deformation, but still elastic with respect to bending and twist. The same remark applies to rupture. Bending about two axes are treated independently. There is no interaction between bending and twisting. Rupture depends on accumulated effective plastic curvature or effective angle of twist per unit length. When the rupture of any member is predicted, that member is considered as inactive member and that member does not contribute to system stiffness or mass.

This moment-curvature, elastic-plastic, beam element model was used in modeling the members of the supporting structures of the transmission line.

6.1 Moment-Curvature Beam Element Model

It is hard to produce an exact behavior of the beam element using an equivalent stress-strain law and the exact cross-sectional properties of the beam members. In practical engineering analysis, the data available for the description of the behavior of the beam members may be given only in the form of the relationships between bending moment and curvature (to describe the flexural behavior) and between torsional moment and angle of twist (to describe the torsional behavior). These relationships are input in ADINA in the form of multi-linear functions (see Figure 6.1). (ADINA, 2003)

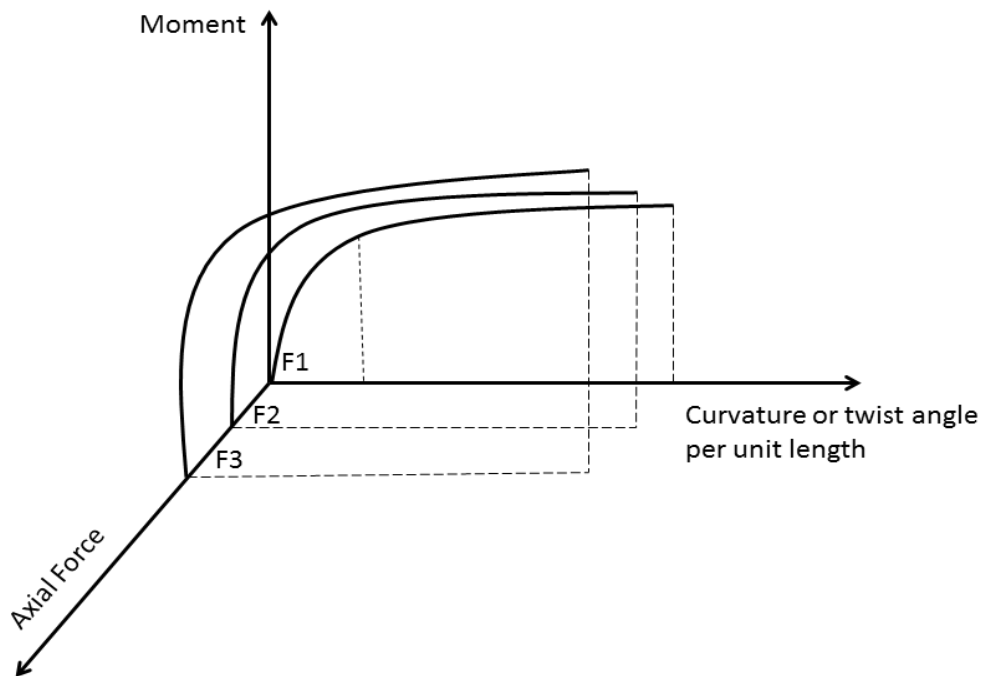


Figure 6.1 ADINA Input Curves for the Moment-Curvature Models

The bending moment vs. curvature and torsional moment vs. angle of twist relationships are functions of axial force and this dependence can be different in tension and compression. In ADINA, the input to bending moment/curvature and torsional moment/twist curves consists for several different levels of axial forces. Therefore, bending moment/curvature and torsional moment/twist for different levels of axial forces are generated using the procedure described in the following sections.

6.2 Determination of Moment-Curvature Relation for Beam Section

In order to use moment-curvature beam elements, one needs to provide the moment-curvature curves for each section that was used in supporting structure for different levels of tensile and compressive axial forces. These moment-curvature curves were generated using the finite element procedure in ADINA.

A finite element model of an L-section was generated, using the plate element, to find the bending moment vs. curvature data. The length of the plate element was considered as 0.5m. A typical model for cross-section L64x64x4.8 is depicted in Figure 6.2. An elastic-perfectly plastic material model was used in this analysis. An elastic-perfectly plastic material shows linear elastic behavior as the load on the structure increases, as long as the stresses are less than the yield strength of the material. Once the stress reaches yield strength of the material, the material undergoes irreversible deformation without any increase in stress.

One end of the finite element model was fixed, while at the free end all the nodes were connected to the centroid of the cross-section using rigid elements and the axial force was applied on the cross section as a distributed load, as shown in Figure 6.2. A static non-linear elastic-plastic analysis was conducted with an applied increasing moment about a reference axis passing through the centroid of the cross section at the free end. The variation of curvature with the applied moment was obtained. Figure 6.3 shows the bending or deformation of the beam section for an axial load of 50 kN.

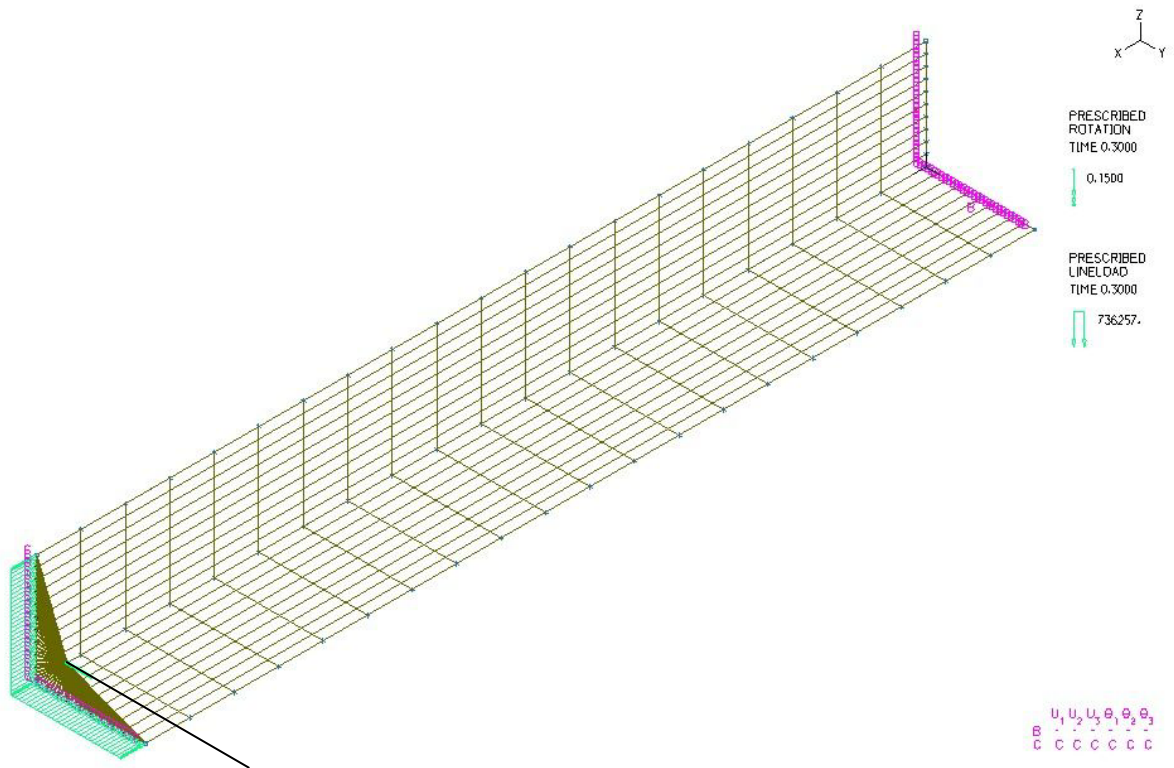


Figure 6.2 Finite Element Model of Cross-Section L64x64x4.8 using the Plate Elements

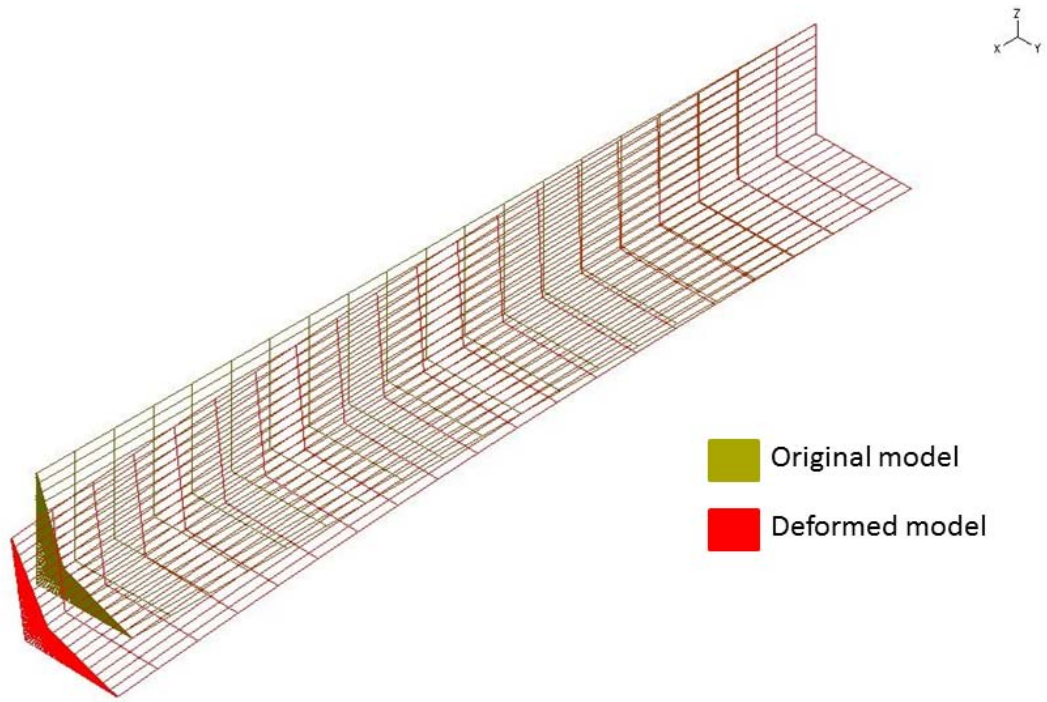


Figure 6.3 Deformed Configuration of the Beam Section due to Moment about Y-axis with an Axial Load

The moment-curvature input data obtained from this analysis for an axial force of 50 kN is given in Table 6.1 and the corresponding moment/curvature plot is presented in Figure 6.4.

Table 6.1 Moment-Curvature data for Section L64x64x4.8 with an axial force of 50 kN

Bending Moment (N-m)	Curvature (Rad/m)
-1760	-0.146
-1620	-0.051
-1320	-0.026
0	0
850	0.015
1250	0.045
1400	0.145

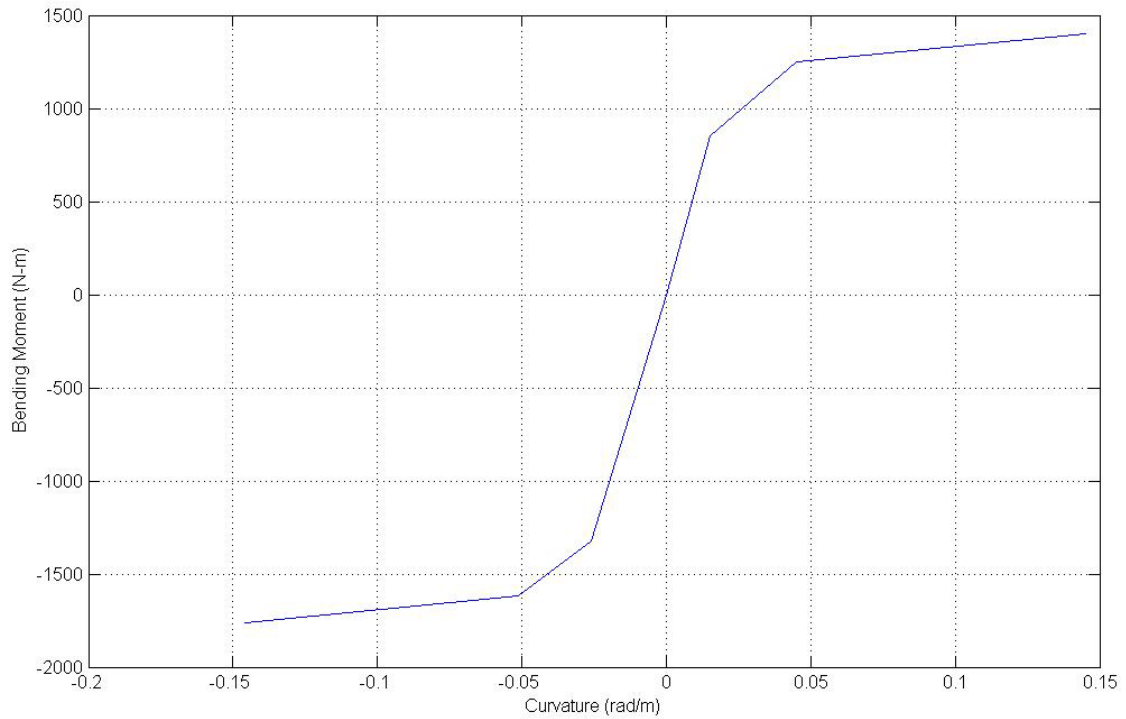


Figure 6.4 Moment-Curvature Relationship (data from Table 6.1) for Section L64x64x4.8

The moments/curvature relationships were generated for each section for different levels of tensile and compressive axial forces, with moments applied about Y and Z axes, passing through the centroid of the cross section using the same procedure as described above.

6.3 Determination of Torque-twist Relation for Beam Section

Another finite element model was generated, using a 3D-solid element, to determine the torsional moment vs. angle of twist data. The length of this solid element was also considered as 0.5m and one end of the model was fixed, as shown in figure 6.3 (for L64x64x4.8 section). At the other end, the surfaces were connected to the centroid of the

cross-section, as shown in Figure 6.5 below. A static non-linear elastic-plastic analysis was conducted with an increasing torque about a reference axis passing through the centroid of the cross section at the free end. The variation of curvature with the applied torque was obtained. Figure 6.6 shows the twisting of the beam section for an axial load of 50kN.

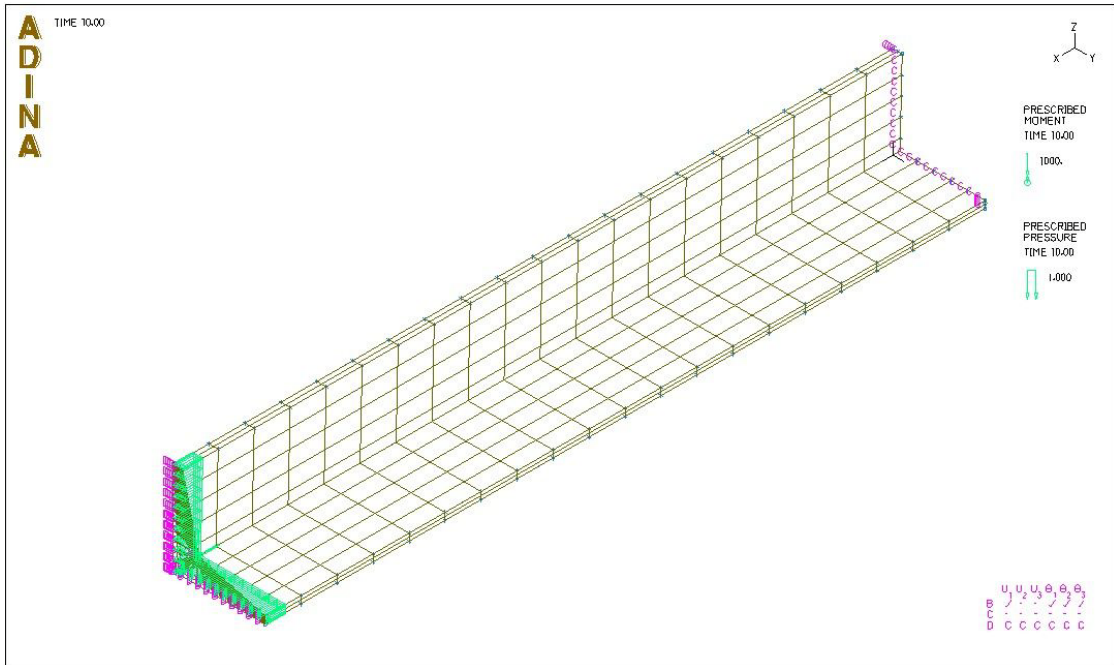


Figure 6.5 Finite Element Model of Cross-Section L64x64x4.8 using the 3D-Solid Element

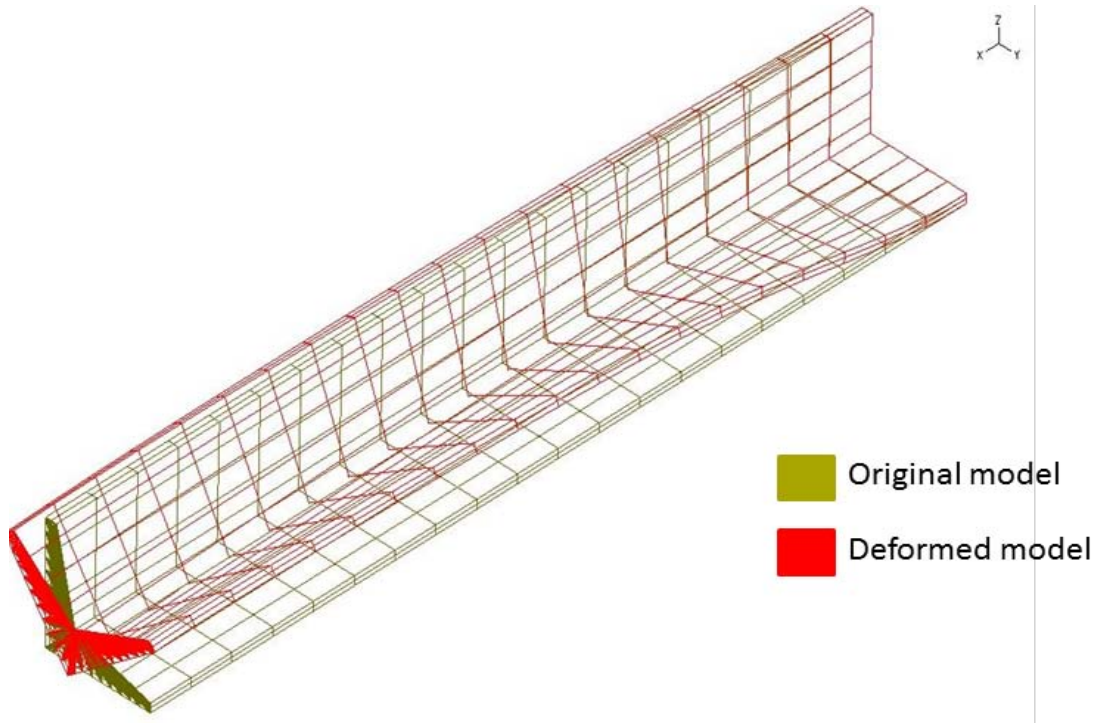


Figure 6.6 Deformed Configuration of the Beam Section due to Torque about X-axis with an Axial Load

The torsional moment-angle of twist input data collected from this test is given in Table 6.2 and the respective input plot is also shown in Figure 6.7.

Table 6.2 Torsional Moment-Angle of Twist data for Section L64x64x4.8 with an axial force of 50kN

Torsional-Moment (N-m)	Angle of Twist (Rad/m)
0	0
200	0.105
310	0.24
380	0.62

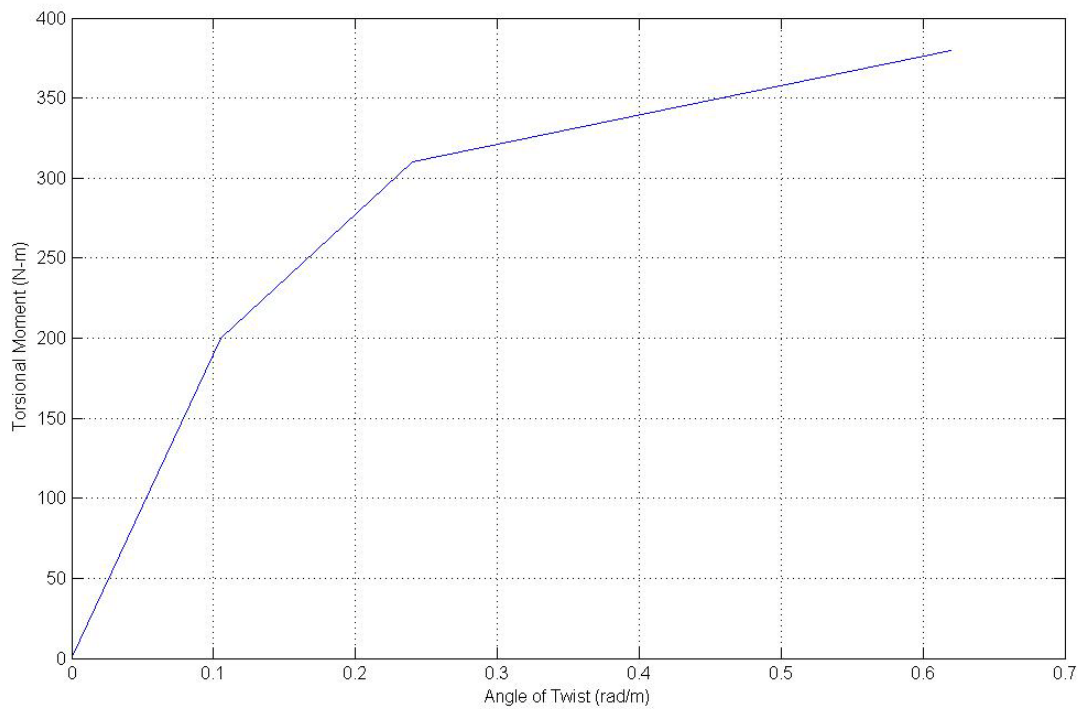


Figure 6.7 Torsional Moment-Angle of Twist Relationship (data from Table 6.1) for Section L64x64x4.8

6.4 Static and Transient Dynamic Analysis of Transmission Line with Broken Conductor for Line Model with Moment-Curvature Element

Using the moment-curvature beam element for the supporting structures, the transmission line system was re-modeled and the following analyses were undertaken.

- Initial static analysis
- Transient dynamic analysis on transmission line modeled with bare conductors when conductors were ruptured in one of the spans.
- Transient dynamic analysis on transmission line modeled with conductors with one-inch radial load when conductors were ruptured in one of the spans.

The procedure for conducting each of these tests was exactly the same as discussed in chapter 5 (5.1 to 5.3). The initial tension in the insulator strings and the conductors were the same; 6.92 kN and 27.87.kN respectively.

6.4.1 Transient Dynamic Analysis for Bare Conductor when Conductors were ruptured

The time history of insulator tension for the insulators on the two towers adjacent to the conductor rupture, for the moment-curvature beam model, is presented in Figure 6.8. The maximum dynamic tensions in the insulator strings on the adjacent towers were extracted from these plots and presented in Table 6.3.

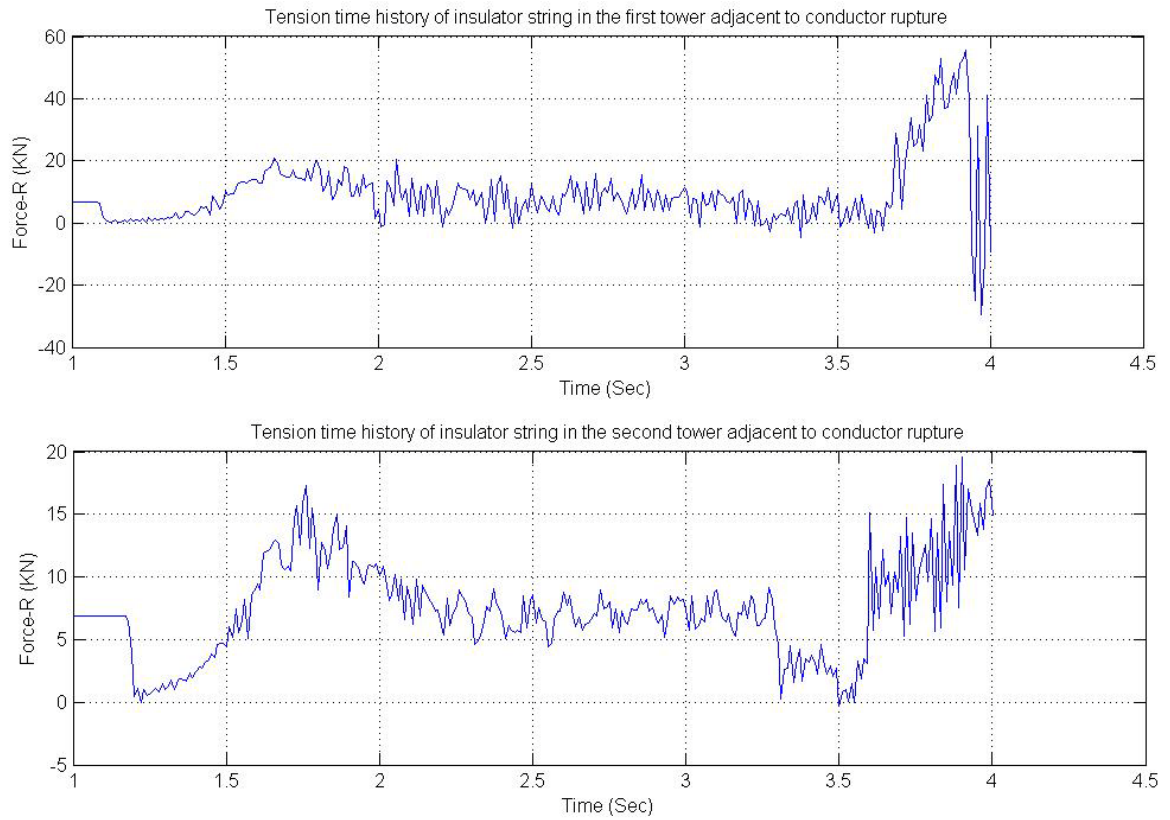


Figure 6.8 Time History of Insulator Tension for the Insulators of Adjacent Towers to Conductor Rupture

Table 6.3 Maximum Dynamic Tensions in Insulator Strings on Adjacent Towers

Insulator string	Maximum dynamic tension in the Line Model (kN)
Insulator string in 1 st tower adjacent to conductor break	20.7
Insulator string in 2 nd tower adjacent to conductor break	19.56
Insulator string in 3 rd tower adjacent to conductor break	14.78
Insulator string in 4 th tower adjacent to conductor break	13.94
Insulator string in 5 th tower adjacent to conductor break	13.59
Insulator string in 6 th tower adjacent to conductor break	13.57

From the simulation analysis, the failed transmission line obtained from the results is presented in Figure 6.9. It can be observed that the two adjacent towers collapsed within a few seconds of the occurrence of conductor rupture and the rest of the towers do not collapse. The first tower adjacent to the span, where conductors rupture was simulated, started to fail at time 3.101th second (see Figure 6.10 and Figure 6.11). The maximum dynamic tension observed in the insulator string before the structure failure is about 20.7kN. The second adjacent tower started to fail at 3.941th second (see Figure 6.12 and Figure 6.13). The maximum dynamic tension in the insulator string of the second adjacent tower, before the tower failure, is 19.56kN. However, the subsequent towers

were still intact and the forces experienced in the insulator strings of these towers decreased, as we moved away from the span where conductors were ruptured.

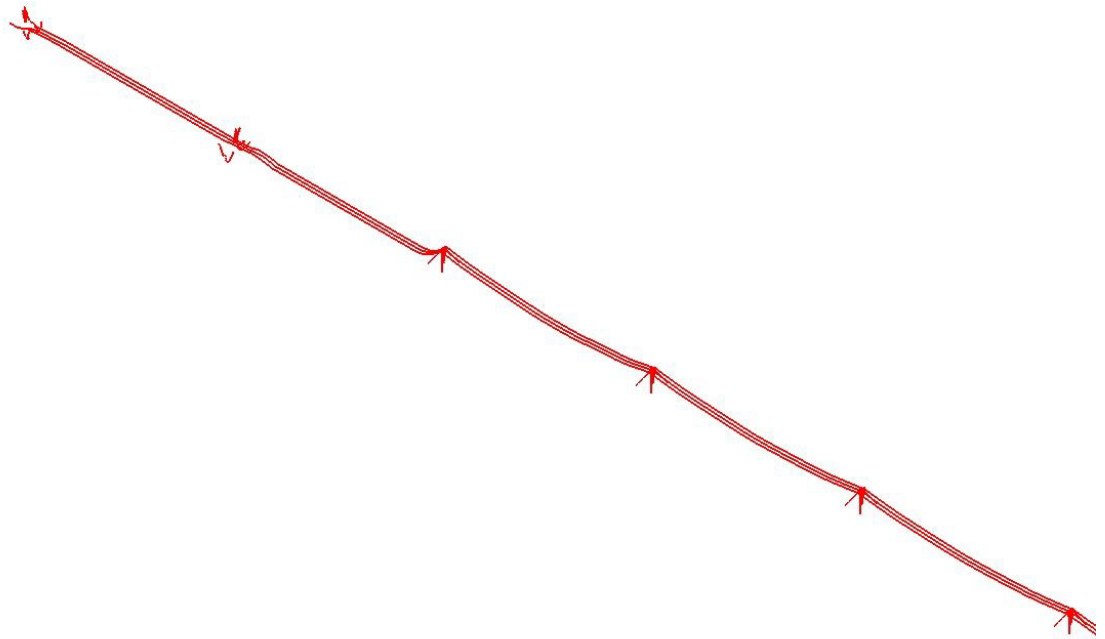


Figure 6.9 Transmission Line Cascade Failure in Two Towers Adjacent to the Span where Conductor Rupture Occurs

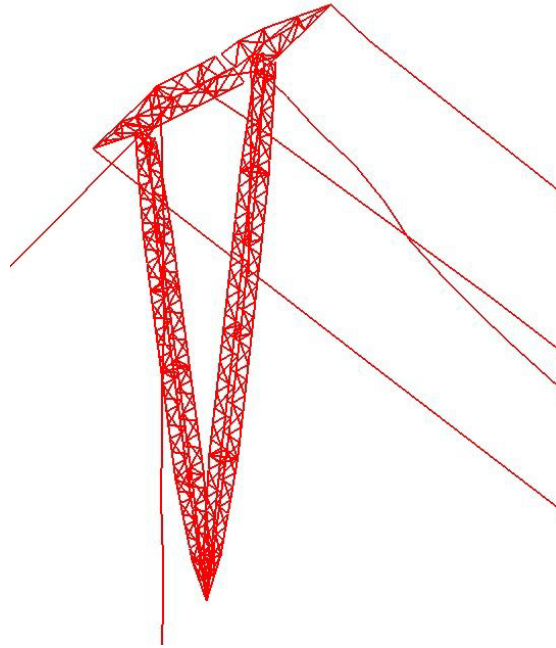


Figure 6.10 Start of failure of members in the first tower adjacent to the span where conductor breakage occurs

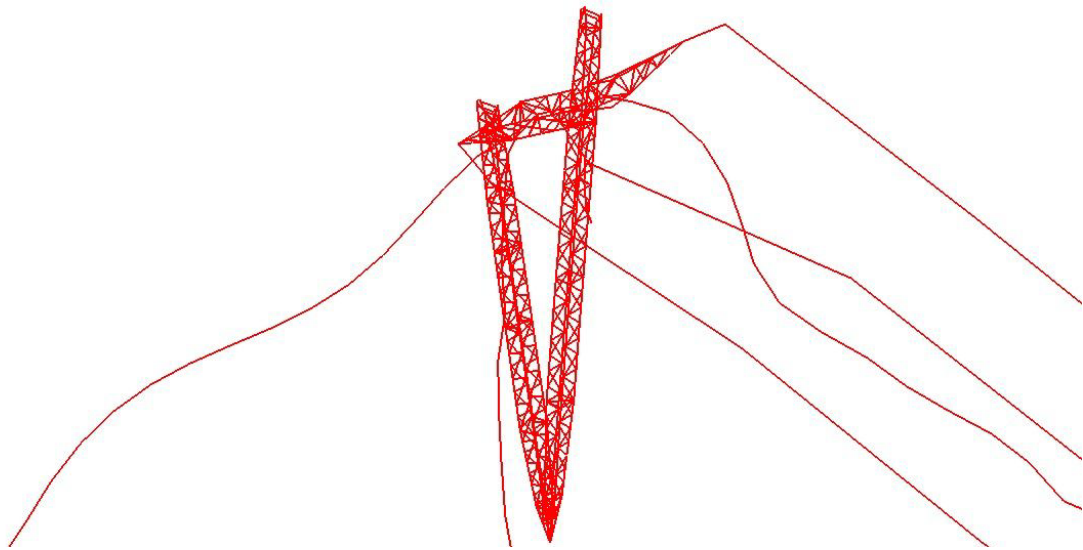


Figure 6.11 First Adjacent Tower Complete Failure

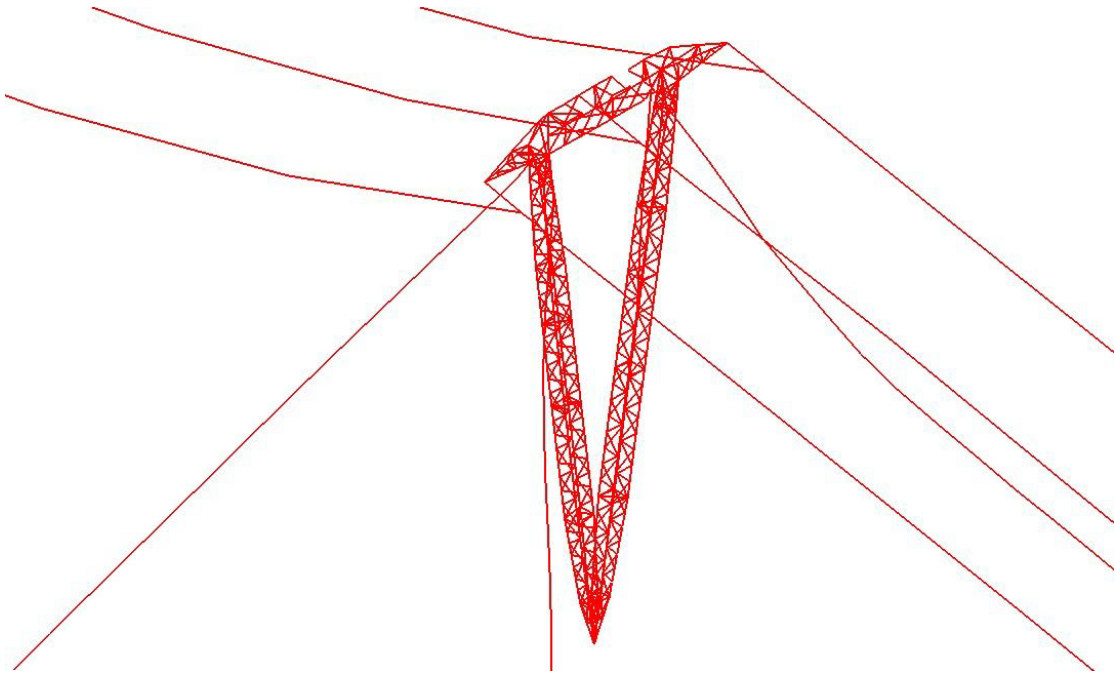


Figure 6.12 Start of failure of members in the second tower adjacent to the span where conductor breakage occurs

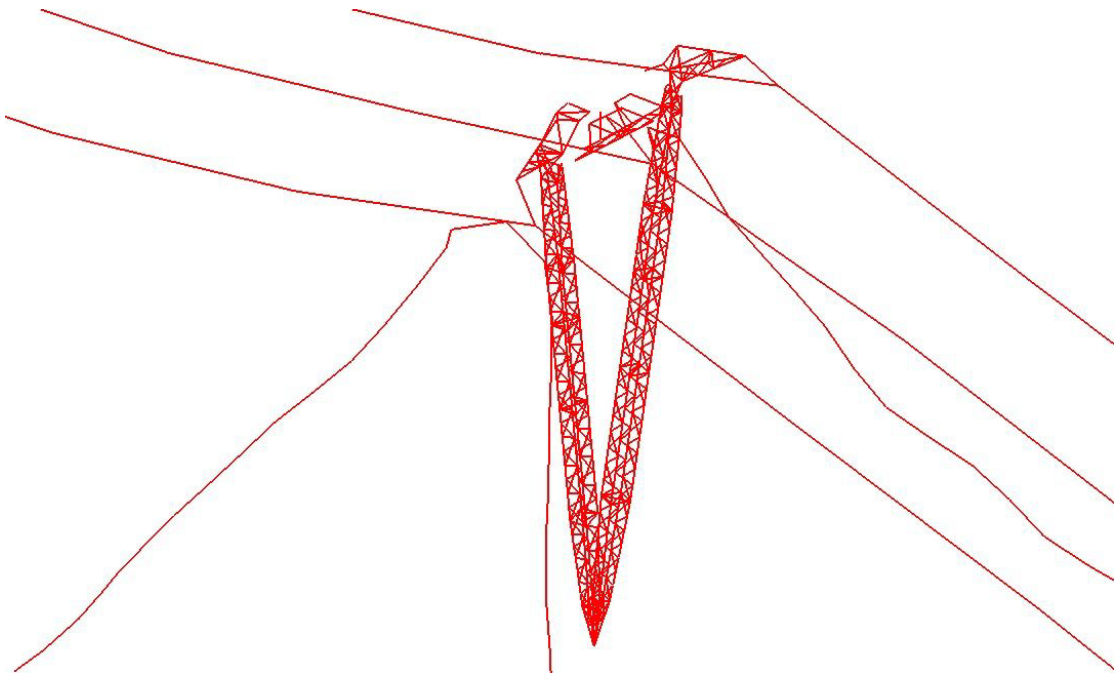


Figure 6.13 Second Adjacent Tower Complete Failure

6.4.2 Transient Dynamic Analysis of transmission line with 1-in radial ice load on conductors with simulated conductor rupture in one of the span

The transient dynamic analysis of transmission line with broken conductors in one span was carried out with 1-inch radial ice load on the conductors. The analysis procedure was same as described in sub-section 5.3. Information extracted from the second static analysis showed that the conductor tension has increased to 72kN, due to the added ice load on the conductor, and the tension in the insulator strings (21.786kN) equals the new conductor weight, including the weight of 1-inch radial ice in the span.

The time history of the insulator string tensions for the insulators in the two adjacent towers can be seen in Figure 6.14. Table 6.4 shows the maximum dynamic insulator string tension in the subsequent towers, extracted from the time history plots.

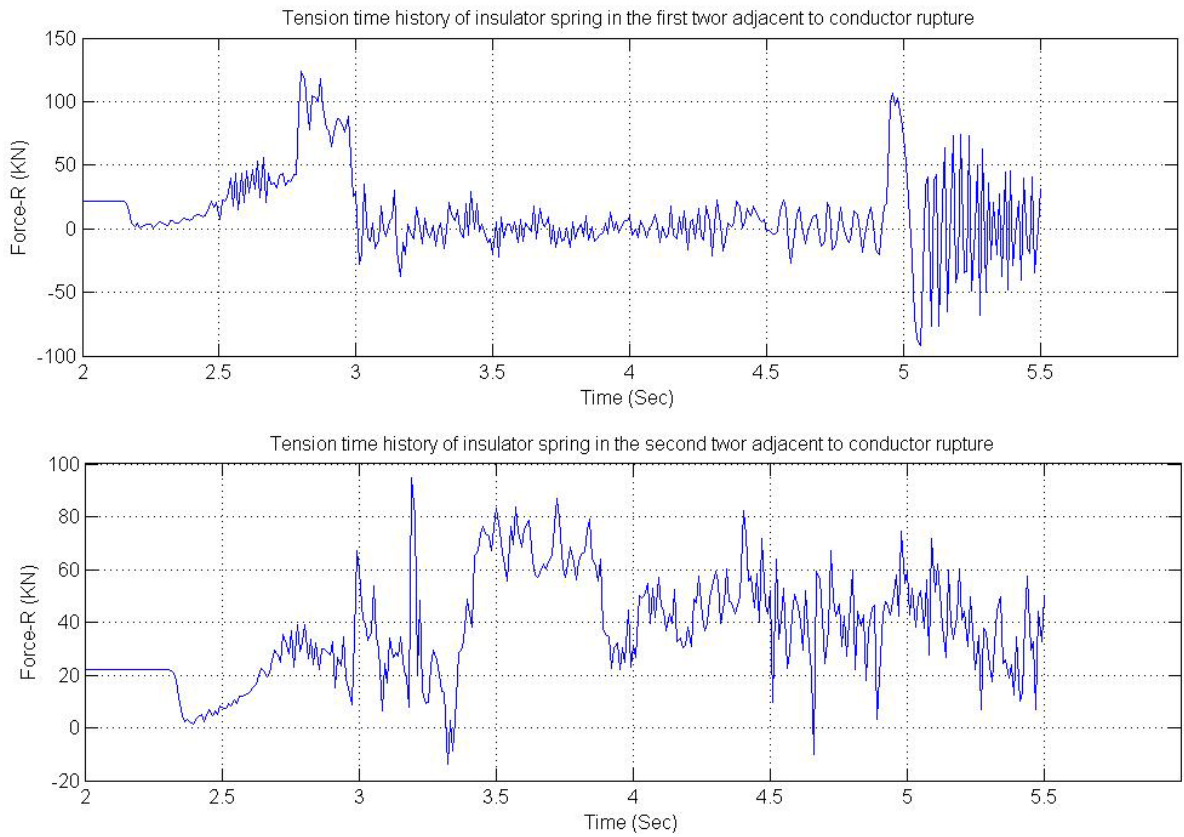


Figure 6.14 Time History of Insulator Tension for the Insulators of Adjacent Towers to Conductor Rupture

Table 6.4 Maximum Dynamic Tensions in Insulator Strings on Adjacent Towers

Insulator String	Maximum Dynamic Tension in the Line (kN)
Insulator string in 1 st tower adjacent to conductor break	21.29
Insulator string in 2 nd tower adjacent to conductor break	39.21
Insulator string in 3 rd tower adjacent to conductor break	52.51
Insulator string in 4 th tower adjacent to conductor break	48.97
Insulator string in 5 th tower adjacent to conductor break	44.04
Insulator string in 6 th tower adjacent to conductor break	42.61
Insulator string in 7 th tower adjacent to conductor break	43.00
Insulator string in 8 th tower adjacent to conductor break	51.51

Eight adjacent towers, on either side of the span, where conductor rupture occurred, have failed completely (see Figure 6.15). The individual failure time of each of these towers is given in Table 6.5. It was observed that the tower failure occurred progressively, with the

towers nearest to the conductor rupture failing first followed by the next closest tower and so on. Clearly, the radial ice loading on the conductors had a significant impact on the length of the cascade failure of transmission line model. The towers, subsequent to the failed towers, remain intact but experience significant tensions (between 40-45kN) in their insulator strings after the cascade failure.

Table 6.5 Tower Failure Time for the Adjacent Towers after Conductor Rupture

Adjacent Tower Number	Failure Time (Sec)
1 st tower adjacent to conductor break	2.471
2 nd tower adjacent to conductor break	2.791
3 rd tower adjacent to conductor break	3.191
4 th tower adjacent to conductor break	3.681
5 th tower adjacent to conductor break	4.161
6 th tower adjacent to conductor break	4.661
7 th tower adjacent to conductor break	5.101
8 th tower adjacent to conductor break	5.701

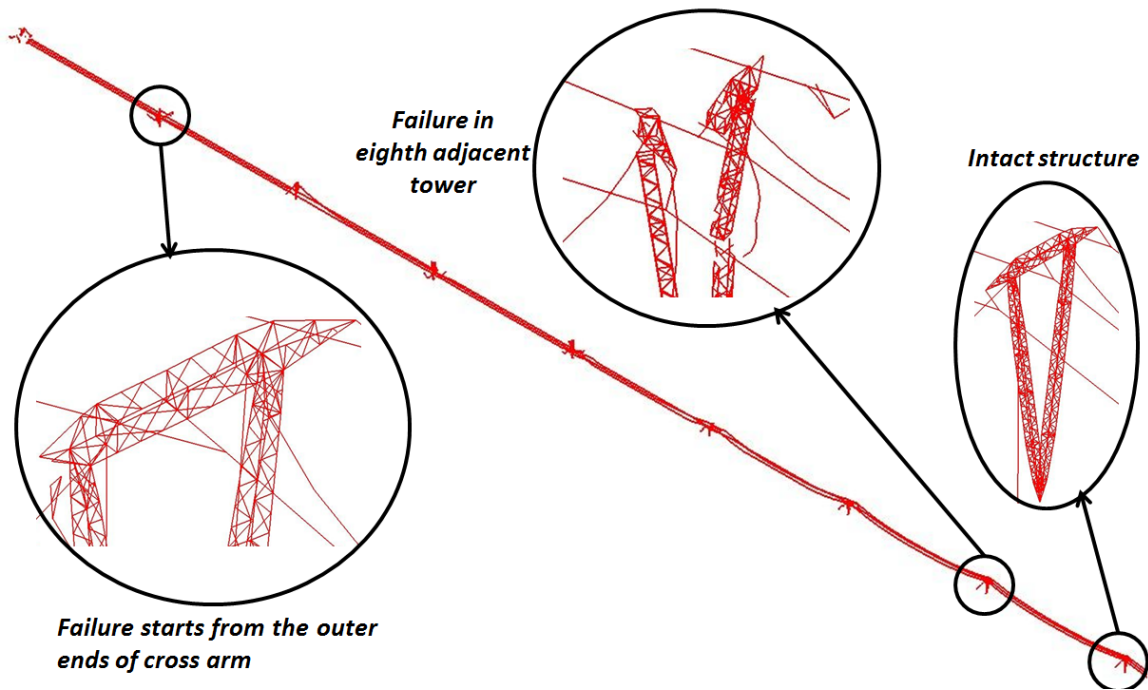


Figure 6.15 Transmission Line Cascade Failure in Eight Towers Adjacent to the Span where Conductor Rupture Occurs

It was observed that the first tower, adjacent to the span, where conductor breakage occurs, behaved in a similar way as in the bare conductor analysis. However, from the second adjacent tower onwards the tower failure behavior was not similar to the bare conductor analysis. Due to the vertical loads exerted by the one-inch radial ice on the conductor and the longitudinal forces in the conductor, the cross-arms experienced the failure process from the outer ends of the arm.

6.5 Closure

Various finite element models were developed to obtain the moment-curvature and torsion-twisting relationships for each cross-section in the supporting towers. Using the data, the transmission line was re-modeled, which included supporting towers with

moment-curvature beam elements. After performing the transient dynamic analyses on the elastic-plastic, moment-curvature beam element model, cascade failure (due to conductor rupture) has been achieved. The bare conductor dynamic analysis has shown that two towers on either ends of the span, where conductors were made to fail, collapse and the radial ice load conductor analysis has proved that if conductors in a span are ruptured, the length of cascade failure was far greater than the one observed in bare conductor analysis. Therefore, in order to reduce the length of cascading in the transmission line, load limiting devices were introduced. The effect of load limiting devices on cascade failure of transmission line conductors has been discussed in the next chapter.

7. Use of Load Limiting Devices

Cascade failure of supporting structures, as seen from the previous section, should be limited to a few structures or prevented if possible. With intact conductors, the supporting structures will see small longitudinal loads during construction. These longitudinal loads are generally much smaller than those that occur when the conductors break. Whenever the conductors break in one span, the supporting adjacent towers experience very high dynamic longitudinal loads, as presented in the previous sections. If the supporting tower adjacent to the span (where the conductors rupture) collapse, the next tower is subjected to high longitudinal loads and may collapse as well. When the conductors rupture, the progressive collapse of more than two or three towers, on either side of the span is called a cascade.

There have been many attempts to develop mechanical cascade prevention devices to limit the dynamic longitudinal loads on the towers. The methods for limiting the dynamic forces can be broadly classified as releasing and sliding clamps, insulator assembly releases, rotating and deformable cross-arms etc. (Peabody and McClure, 2002). In general, all these mechanical devices can be called Load Control Devices. Load control devices can be grouped into four groups-

- Load Limiting Devices- At a predetermined load, the device fail or slip, releasing the force acting on the tower.
- Force Reduction Devices- These devices have both force limiting and energy absorbing characteristics.

- Structure based force control methods
- Load Removal Devices

In order to study the effectiveness of Load Reduction Devices, ANCO Tower Load Controller (TLC) (ANCO, 1989) was chosen. The device consists of two flat plates bolted together. These plates are flame cut in such a way as to allow them to extend like a double-coil helix spring. In the event of a dynamic shock that could cause a tower to fail, the device extends up to two meters (6.6 feet), to absorb shock energy and limit the force applied to the tower.

The load-deformation characteristics of this device (ANCO, 1989) was digitized and presented in Figure 7.1. In the present analysis, this ANCO TLC was modeled as a non-linear spring.

The transmission lines that were used before were re-modeled by introducing the non-linear spring between the insulator spring and the tower cross-arm. The transient dynamic analyses were performed to study the effect of TLC on the longitudinal forces and collapse of the tower.

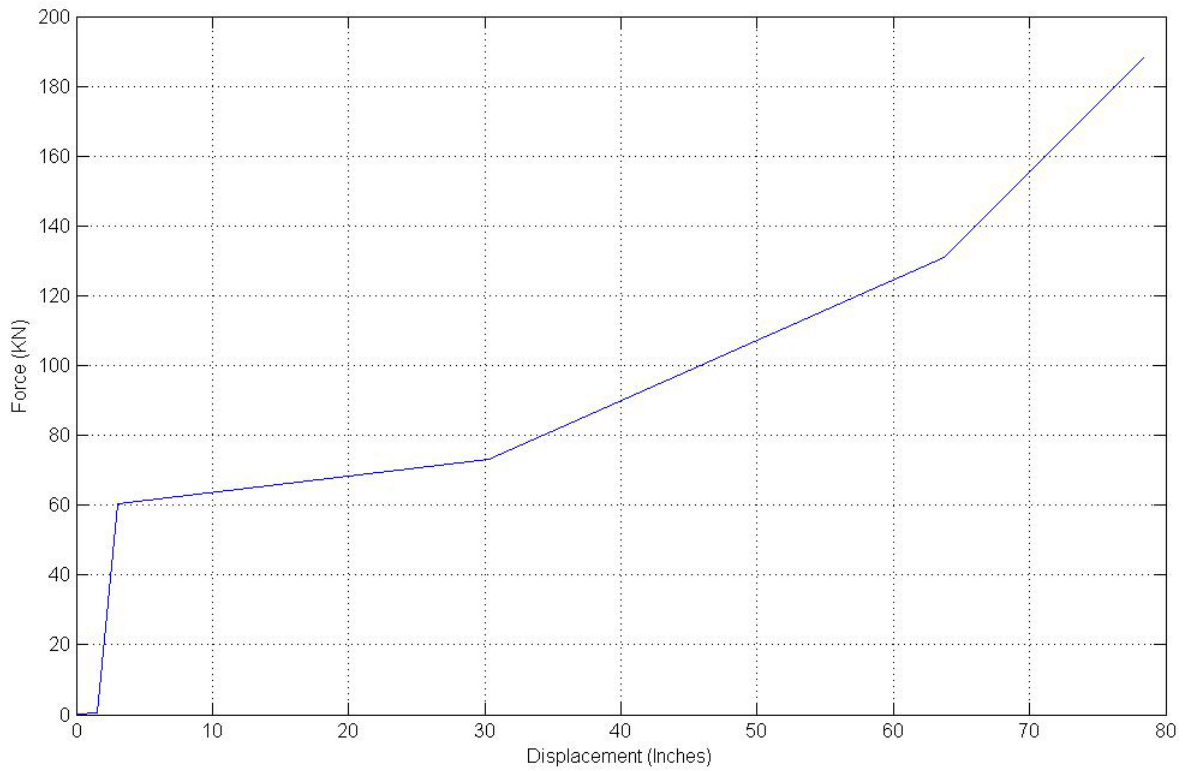


Figure 7.1 Load-Deformation Characteristic of TLC

7.1 Analyses of Intact Towers

The transient dynamic analyses were conducted on the line models, where the towers are modeled using linear elastic material. The tension in the insulator string reduced considerably as seen in tables 7.1 to 7.4.

Table 7.1 Comparison of the Tension in Insulator Strings of the Truss Model with Bare Conductor

Tower Number	Maximum Tension in Insulator (Without TLC) (kN)	Maximum Tension in Insulator (With TLC) (kN)
Insulator string in 1 st tower adjacent to conductor break	45.40	31.42
Insulator string in 2 nd tower adjacent to conductor break	20.88	17.98
Insulator string in 3 rd tower adjacent to conductor break	17.33	16.24
Insulator string in 4 th tower adjacent to conductor break	15.89	15.19
Insulator string in 5 th tower adjacent to conductor break	14.82	14.26

Table 7.2 Comparison of the Tension in Insulator Strings of the Truss Model with 25 mm (i-in.) radial Ice Loaded Conductor

Tower Number	Tension in Insulator (Without TLC) (kN)	Tension in Insulator (With TLC) (kN)
Insulator string in 1 st tower adjacent to conductor break	97.73	67.46
Insulator string in 2 nd tower adjacent to conductor break	64.12	40.16
Insulator string in 3 rd tower adjacent to conductor break	43.33	33.53
Insulator string in 4 th tower adjacent to conductor break	40.06	30.89
Insulator string in 5 th tower adjacent to conductor break	36.86	30.28

Table 7.3 Comparison of the Tension in Insulator Strings of the Linear Material Beam Model with Bare Conductors

Tower Number	Tension in Insulator (Without TLC) (kN)	Tension in Insulator (With TLC) (kN)
Insulator string in 1 st tower adjacent to conductor break	48.32	31.46
Insulator string in 2 nd tower adjacent to conductor break	22.99	19.05
Insulator string in 3 rd tower adjacent to conductor break	17.80	15.92
Insulator string in 4 th tower adjacent to conductor break	15.49	15.12
Insulator string in 5 th tower adjacent to conductor break	15.13	14.45

Table 7.4 Comparison of the Tension in Insulator Strings of the Linear Material Beam Model with Ice Loaded Conductors

Tower Number	Tension in Insulator (Without TLC) (kN)	Tension in Insulator (With TLC) (kN)
Insulator string in 1 st tower adjacent to conductor break	112.29	66.86
Insulator string in 2 nd tower adjacent to conductor break	57.91	39.94
Insulator string in 3 rd tower adjacent to conductor break	51.59	33.84
Insulator string in 4 th tower adjacent to conductor break	43.85	31.26
Insulator string in 5 th tower adjacent to conductor break	41.61	30.35

The comparative dynamic force time history response of the insulator strings, of the radial ice loaded conductor models, where maximum dynamic tension is experienced is given in Figure 7.2 and Figure 7.3.

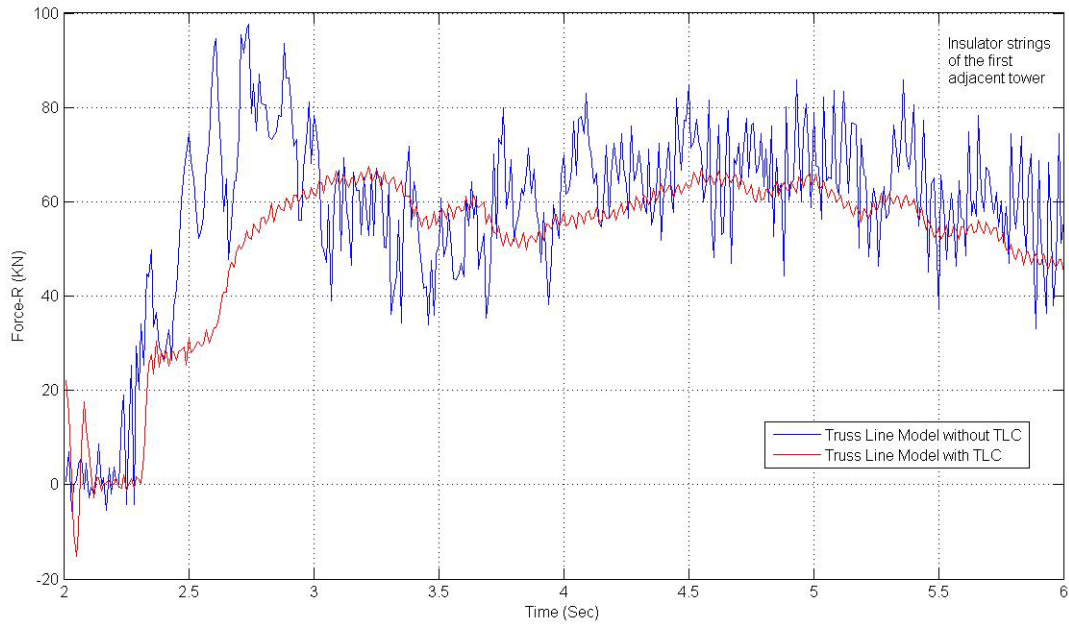


Figure 7.2 Time History Response of the Insulator Strings in Truss Line Model with Radial Ice Load

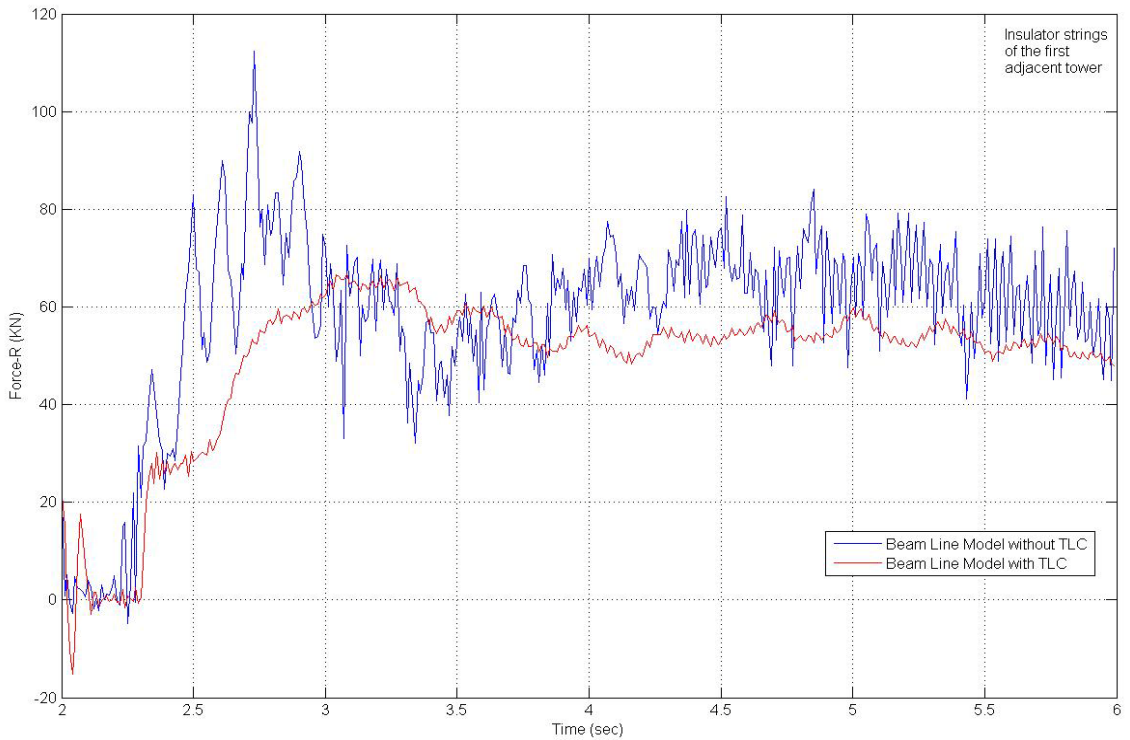


Figure 7.3 Time History Response of the Insulator Strings in Beam Line Model with Radial Ice Load

7.2 Collapse Analysis of Transmission Line Model with TLC

The transient dynamic analyses were conducted on transmission line models, where the tower members were modeled using elasto-plastic material model.

7.2.1 Dynamic Analysis of Transmission Line Model with Bare Conductors

With TLC introduced between the insulator and cross-arm of the structure, two towers adjacent to the span, where the conductors were ruptured, collapsed as in the case without TLC, but, insulator tensions were decreased. The dynamic force history in the insulator string of the tower adjacent to the span, where conductors were cut, is presented in Figure 7.4 and the maximum insulator forces in adjacent towers are given in Table 7.5.

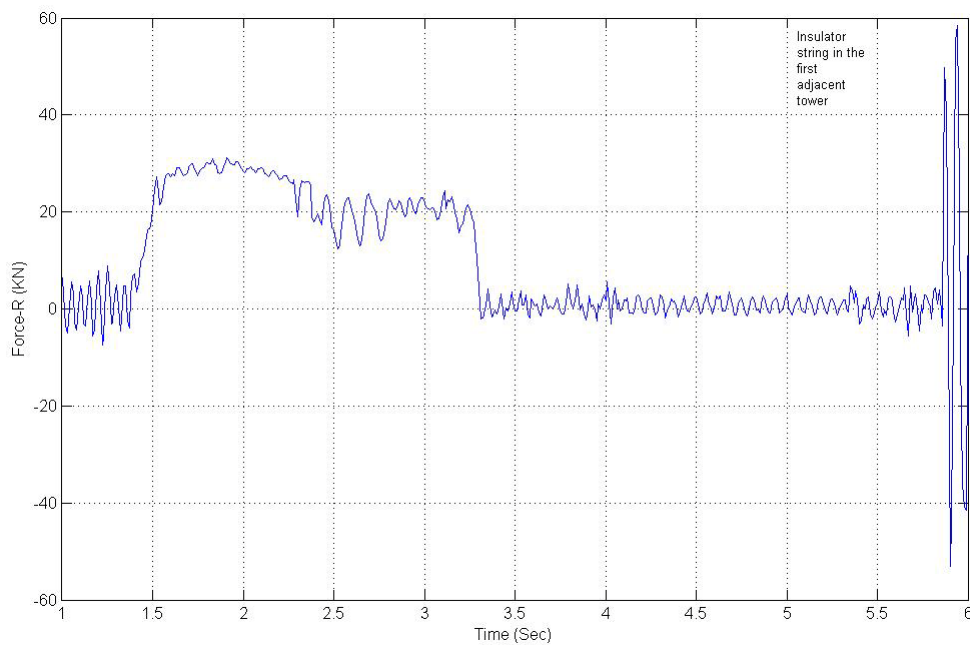


Figure 7.4 Force History of the Insulator String in the First Tower, adjacent to the Conductor Failure Span, of the Moment-Curvature Beam Line with TLC and Bare Conductors

Table 7.5 Maximum Insulator Forces in Adjacent Towers in M-C Beam Model with Bare Conductors

Tower Number	Tension in Insulator (Without TLC) (kN)	Time of Tower Failure (Sec)	Tension in Insulator (With TLC) (kN)	Time of Tower Failure (Sec)
Insulator string in 1 st tower adjacent to conductor break	41.00	3.081	31.13	3.241
Insulator string in 2 nd tower adjacent to conductor break	20.7	3.931	16.75	5.311
Insulator string in 3 rd tower adjacent to conductor break	19.56	-	13.45	-
Insulator string in 4 th tower adjacent to conductor break	14.78	-	12.91	-
Insulator string in 5 th tower adjacent to conductor break	13.94	-	12.26	-

7.2.2 Dynamic Analysis of Transmission Line Model with 25mm (1-inch) Radial Ice Load

With radial ice load, without TLC device, eight adjacent towers collapsed, whereas with TLC device connected, only three towers adjacent to the span, where the conductors were ruptured, collapsed (see Figure 7.5). Therefore, one can see that with TLC, the length of

cascade can be reduced. The maximum insulator forces in adjacent towers are shown in Table 7.6.

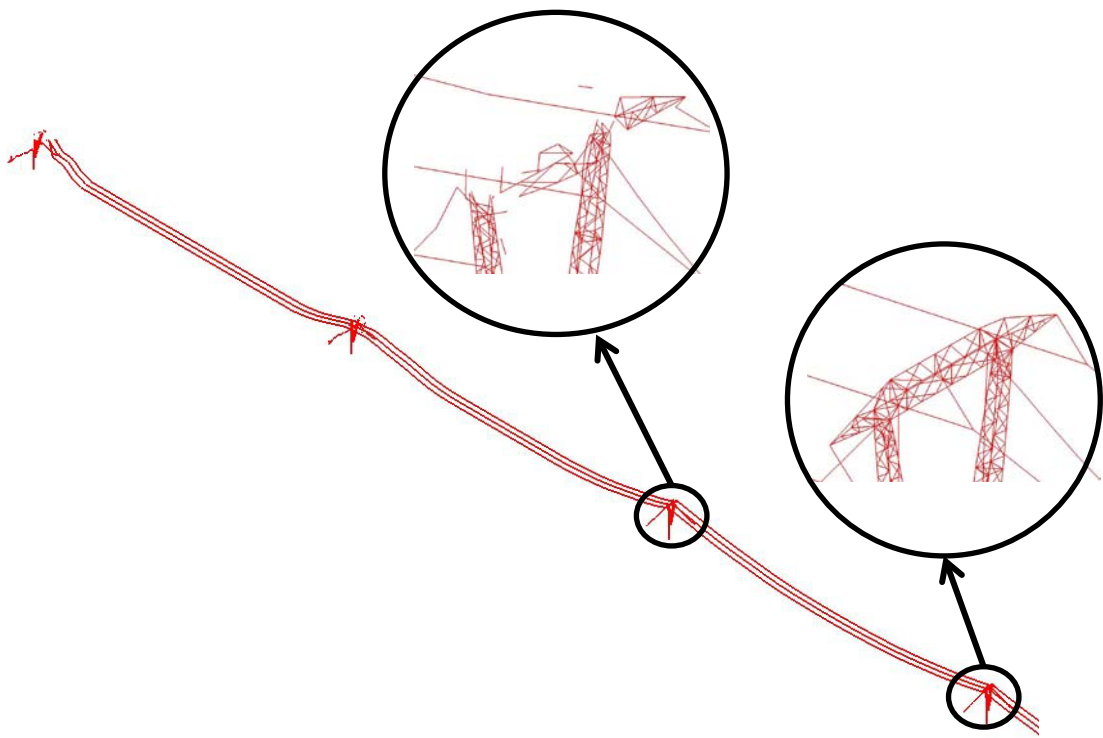


Figure 7.5 Transmission Line Section with Radial Ice Load

Table 7.6 Maximum Insulator Forces in Adjacent Towers in M-C Beam Model with Ice Loaded Conductors

Tower Number	Tension in Insulator (Without TLC) (kN)	Time of Tower Failure (Sec)	Tension in Insulator (With TLC) (kN)	Time of Tower Failure (Sec)
Insulator string in 1 st tower adjacent to conductor break	50.85	2.471	47.34	2.711
Insulator string in 2 nd tower adjacent to conductor break	46.69	2.791	45.39	3.221
Insulator string in 3 rd tower adjacent to conductor break	67.208	3.191	46.34	3.981
Insulator string in 4 th tower adjacent to conductor break	40.97	3.681	27.73	-
Insulator string in 5 th tower adjacent to conductor break	48.97	4.161	27.61	-
Insulator string in 6 th tower adjacent to conductor break	44.04	4.661	27.77	-
Insulator string in 7 th tower adjacent to conductor –break	42.61	5.101	27.95	-
Insulator string in 8 th tower adjacent to conductor break	43.00	5.701	28.18	-

The time history response for insulator strings in the first tower adjacent to the span, where conductor rupture is simulated, for both the models can be compared from Figure 7.6.

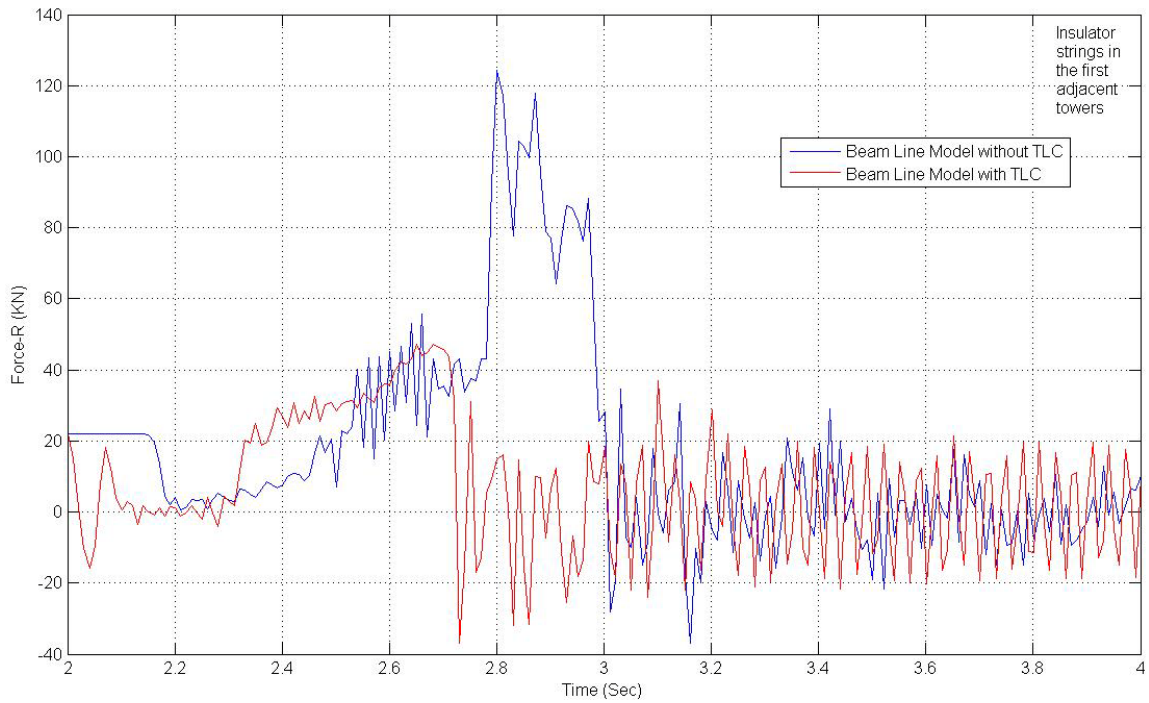


Figure 7.6 Comparative Force History of the Insulator String in the First Tower, adjacent to the Conductor Failure Span, of the Moment-Curvature Beam Line (with and without TLC) with Radial Ice Load

7.3 Closure

Using the load-deformation characteristics (Figure 7.1) of the ANCO Tower Load Controller (ANCO, 1989), a non-linear spring was introduced between the cross-arm and the insulator strings of the supporting towers of the transmission line. Comparing the force history of the insulator strings in the first tower, adjacent to the span where

conductor rupture occurred, for the radial ice loaded condition from the linear material models, it has been noted that the dynamic tensions in the insulators have significantly reduced (see Figure 7.2 and Figure 7.3). Also, in the moment-curvature beam element model, TLCs have shown to decrease the length of cascade failure to a great extent, for the 1-in radial ice load scenario, by decreasing the dynamic tension in the insulator strings of the undamaged supporting towers (see Table 7.6).

8. Conclusion

The dynamic behavior of supporting towers and the dynamic forces acting in the adjacent supporting towers, due to conductor rupture in the middle span, have been studied. The results obtained from this linear elastic material model show that the bridge members in the cross-arms exceed the yield strength of the material, after the insulator strings attain the maximum dynamic tension. The transmission line towers were modeled with linear material properties, hence they do not show cascade failure, because the element members are considered to be intact, even upon experiencing large tensions or forces.

To conduct a more realistic cascade failure analyses, a finite element model of the transmission line, with moment-curvature beam elements for the supporting towers, was generated. For this model, the moment-curvature and torque-twist relationships for all the cross-sectional areas of the tower were determined for incremental values of axial loads. It was found that the two towers collapsed on either side of the span, when bare conductors, of the middle span, were ruptured. When the conductors (in the middle span) covered with one-inch radial ice were ruptured, eight towers on either side of the middle span, collapsed. In both these cases, the maximum tensions in the insulator strings were observed to be considerably low when compared to the linear material model analyses.

In order to reduce the length of cascade failure, tower load controllers (TLCs) were introduced to the linear truss and beam line models and the moment-curvature beam model. On performing the transient dynamic analyses on each of these models, it has been observed that the length of the cascade failure remained the same for the bare

conductor analyses, as in moment-curvature beam line model; however the length of cascading has significantly decreased for the 25-mm (1-in) radial ice load scenario. In this case only three adjacent towers, instead of eight, on either side of the span where conductors were ruptured, failed. Also, it was noted that the maximum dynamic tension in the insulator strings had significantly reduced in all the three transmission line models, because the TLCs had the capacity to extend up to two meters when subjected to longitudinal loads.

With all the analytical data generated, the following conclusions were made:

- The cross-arm bridge members experience forces greater than the yield strength of the material; hence it was the weakest supporting section of the transmission line system and was observed to be the epicenter of the supporting tower failure.
- The type of element and material used in modeling the transmission line towers effects the dynamic forces acting on the supporting structures. In case of non-linear material models, the forces experienced by the subsequent towers was more compared to the ones observed in the linear material models.
- The transmission line system, modeled with moment-curvature beam tower elements and TLCs, experienced the least dynamic tensions in the insulator strings. Hence, the TLCs acted as good damper by absorbing significant dynamic forces and bringing down the impact forces on subsequent towers in the line.

9. Recommendations for Future Work

- There has not been any consideration of wind gusts in this study. It would be ideal to include these loads and test the effect of wind gust loading on the cascading of these transmission line models.
- The combined or mixed model, where the column and main cross-arm elements are considered as beam elements and the cross-bracings are considered as truss elements, will need attention.
- This study has only utilized ANCO TLC as a load limiting device. There are several other load limiting devices which could be incorporated to check the effectiveness of those load limiting devices on reducing the dynamic loads on supporting structures and on cascade of transmission towers.

References

“V-type guyed tower”, photo, mannvit engineering (2013). Retrieved 03/10, 2013, from

<http://www.mannvit.com/PowerTransmissionDistribution/Transmissionlinetowers/>

ADINA (automatic dynamic incremental nonlinear analysis) (2003). (V8.6 ed.). Watertown, MA: ADINA R&D Inc.

Applying Rayleigh damping to a model. Retrieved 05/13, 2013, from http://download.autodesk.com/us/algorithm/userguides/mergedProjects/setting_up_the_analysis/nonlinear/Analysis_Parameters/Applying_Rayleigh_Damping_to_a_Model_1_%28Nonlinear%29.htm

Breau, M. (2006). The Quebec ice storm of 1998. Retrieved 03/21, 2013, from <http://icestormof1998.tripod.com/index.html>

Breau, M. (2006). The Quebec ice storm of 1998. Retrieved 03/21, 2013, from <http://icestormof1998.tripod.com/id14.html>

Cohen, E., and Perrin, H. (1957). Design of multi-level guyed towers: Wind loading. *Journal of the Structural Division*, 83(ST5), 1355-1-1355-29.

da Silva, J., Vellasco, P., de Andrade, S., and de Oliveira, M. (2005). Structural assessment of current steel design models for transmission and telecommunication towers. *Journal of Constructional Steel Research*, 61, 1108-1134.

de Oliveira, M., da Silva, J., Vellasco, P., de Andrade, S., and de Lima, L. (2007). Structural analysis of guyed steel telecommunication towers for radio antennas. *Journal of the Brazilian Society of Mechanical Sciences and Engineering*, 29(2), 185-195.

DiGioia, A., Jr., Hirany, A., Newman, F. B., and Rose, A. T. (1998). Rock-socketed drilled shaft design for lateral loads [overhead power line foundations]. Paper presented at the *Transmission & Distribution Construction, Operation & Live-Line Maintenance Proceedings, 1998. ESMO '98. 1998 IEEE 8th International Conference on*, 62-68. doi:10.1109/TDCLLM.1998.668333

Dunford, J. (2011). *Dynamic response analysis of transmission towers after conductor breakage using ADINA*. M. Eng. Thesis. Memorial University of Newfoundland, St. John's, Canada.

Fekr, M., and McClure, G. (1998). Numerical modelling of the dynamic responses of ice-shedding on electrical transmission lines. *Atmospheric Research*, 46(1-2), 1-11.

Gupta, S., Wipf, T., Fanous, F., Baenziger, M., and Hahm, Y. (1994). Structural failure analysis of 345kV transmission line. *IEEE Transactions on Power Delivery*, 9(2), 894.

Kahla, N. (1995). Equivalent beam-column analysis of guyed towers. *Computers & Structures*, 55(4), 631-645.

Kempner, L. J. (1997). *Longitudinal impact loading on electrical transmission line towers: A scale model study*. (PhD Thesis, Portland State University).

Lindsey, K. (1978). Mathematical theory of longitudinal loaded elastic-plastic transmission lines- statics. *IEEE Transactions on Power Apparatus and Systems, PAS-97(2)*, 574.

Lummis, J. and Fiss, R. (1969). Effect of conductor imbalance on flexible transmission structures. *IEEE Transactions on Power Apparatus and Systems, PAS-88(11)*, 1672.

Madugula, M., Wahba, Y., and Monforton, G. (1998). Dynamic response of guyed masts. *Engineering Structures, 20(12)*, 1097-1101.

Mathur, R., Shah, A., Trainor, P., and Popplewell, N. (1987). Dynamics of a guyed transmission tower system. *IEEE Transactions on Power Delivery, PWRD-2(3)*, 908.

McClure, G., and Tinawi, R. (1987). Mathematical modeling of the transient response of electric transmission lines due to conductor breakage. *Computers & Structures, 26(1/2)*, 41-56.

McClure, G., and Lapointe, M. (2003). Modeling the structural dynamic response of overhead transmission lines. *Computers & Structures, 81*, 825-834.

Meshmesha, H., Sennah, K., and Kennedy, J. B. (2003). Beam-column analysis of guyed masts. Paper presented at the *Canadian Society for Civil Engineering - 31st Annual Conference: 2003 Building our Civilization, June 4, 2003 - June 7, Moncton, NB, Canada. , 2003* 1096-1103.

Mozer, J., Wood, W. and Hribar, J. (1981). Broken wire tests on a model transmission line system. *IEEE Transactions on Power Apparatus and Systems, PAS-100*(3), 938.

Munaswamy, K. and Dunford, J. (2013). *Benchmark study for a line modelled in ADINA*. (Tech. Rep No. T063700-3339). Montreal: CEATI International, Inc.

Munaswamy, K. and Haldar, A. (1997). *Mechanical characteristics of conductors with circular and trapezoidal wires*. (Technical No. 319 T 883). Montreal, Quebec: Canadian Electricity Association.

Ostendorp, M. (1998). Longitudinal loading and cascading failure assessment for transmission line upgrades. Paper presented at the *Transmission & Distribution Construction, Operation & Live-Line Maintenance Proceedings, 1998. ESMO '98. 1998 IEEE 8th International Conference on*, 324-329. doi: 10.1109/TDCLLM.1998.668399

Peabody, A. B., and McClure, G. (2002). Load limiters for overhead lines. *4th Structural Specialty Conference of the Canadian Society for Civil Engineering*, Montreal, Quebec, Canada.

Peyrot, A., Kluge, R. and Lee, J. (1980). Longitudinal loads from broken conductors and broken insulators and their effect on transmission lines. *IEEE Transactions on Power Apparatus and Systems, PAS-99*(1), 222.

Richardson, A. (1987). Longitudinal dynamic loading of a steel pole transmission line. *IEEE Transactions on Power Delivery, PWRD-2*(2), 425.

Roy, S., Fang, S., and Rossow, E. (1984). Secondary stresses on transmission tower structures. *Journal of Energy Engineering, 110*(2), 157-172.

Strauss, G., Rice, D., and McCoy, K. (2013, 02/09). *Massive power outages as northeast blizzard turns deadly. USA Today*. Retrieved from.

<http://www.usatoday.com/story/weather/2013/02/08/northeast-new-england-blizzard/1900077/>

Szczecin experiences major power outage. (2013, 04/09). The Warsaw Voice.

Retrieved from

<http://www.warsawvoice.pl/WVpage/pages/articlePrint.php/5995/news>

The Technical Staff, ANCO Engineers, Inc. (1989). *Test verification of a device for reduction of severe dynamic loads in electric transmission towers. prepared for united states department of energy, Oakland, California.* (Technical Report No. 1354.14). Los Angeles, CA, USA: ANCO Engineers, Inc.

Thomas, M., and Peyrot, A. (1982). Dynamic response of ruptured conductors in transmission lines. *IEEE Transactions on Power Apparatus and Systems, PAS-101*(9), 3022.

Tucker, K. (2007). *Validation of full-scale and small-scale transmission line test results on dynamic loads with numerical modeling*. M. Eng. Thesis. Memorial University of Newfoundland, St. John's, Canada.

Whiteway, K. (2005). *Newfoundland power 2007 capital budget documentation: transmission line rebuild strategy*. Retrieved 03/10, 2013, from <http://www.pub.nf.ca/np2007cap/appdivided.htm>

Wikipedia: The free encyclopedia. (2013). *List of power outages*. Retrieved 03/10, 2013, from http://en.wikipedia.org/wiki/List_of_power_outages#Largest

Wikipedia: The free encyclopedia. (2013). *North American ice storm of 1998*. Retrieved 03/10, 2013, from http://en.wikipedia.org/wiki/North_American_ice_storm_of_1998#Impact

Williamson, R. A., and Margolin, M. N. (1966). Shear effects in design of guyed towers. *Journal of the Structural Division, Proceedings of the American Society of Civil Engineers*, 92(ST5), 213-235.

Yang Jingbo, and Li Zheng. (2008). Calculation of wind-induced dynamic load of transmission tower considering coupled vibration affection of conductors. Paper presented at the *Electricity Distribution, 2008. CICED 2008. China International Conference on*, 1-5. doi:10.1109/CICED.2008.5211777

Yang Jingbo, and Li Zheng. (2008). Calculation of wind-induced dynamic load of transmission tower considering coupled vibration affection of conductors. Paper presented at the *Electricity Distribution, 2008. CICED 2008. China International Conference on*, 1-5. doi:10.1109/CICED.2008.5211777